CHALMERS
UNIVERSITY OF TECHNOLOGY

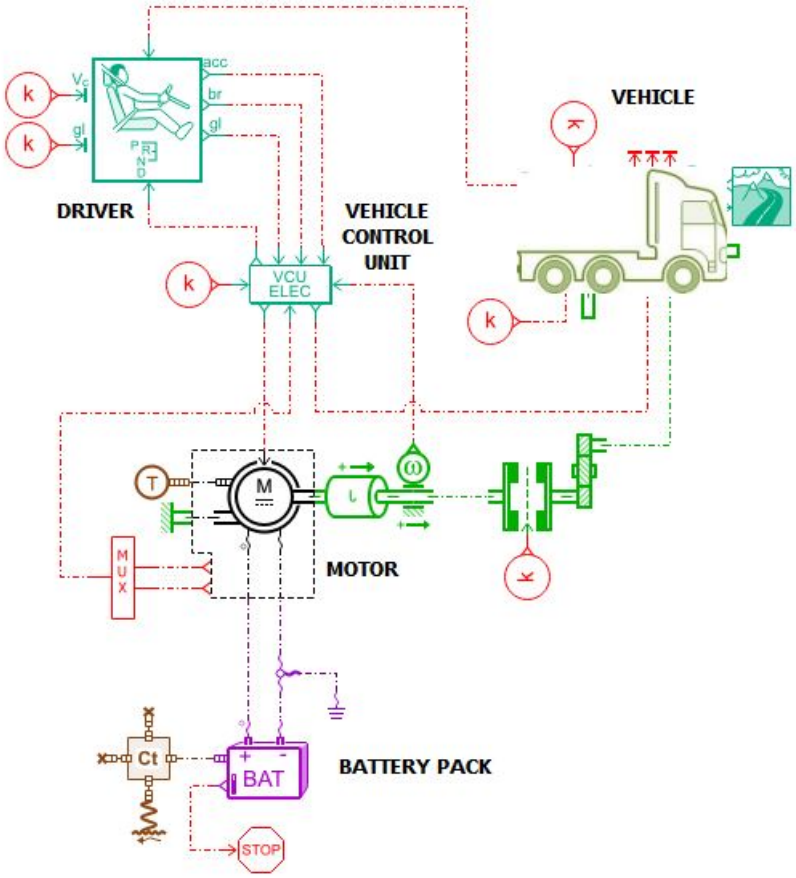

Optimal Control of Reconfigurable Multi-battery Systems

Master's thesis in MPSYS

Nauman Khurshid Haider

DEPARTMENT OF ELECTRICAL ENGINEERING

CHALMERS UNIVERSITY OF TECHNOLOGY
Gothenburg, Sweden 2022
www.chalmers.se

Master's thesis 2022

Optimal control of reconfigurable multi-battery systems

NAUMAN KHURSHID HAIDER

CHALMERS
UNIVERSITY OF TECHNOLOGY

Department of Electrical Engineering
Systems and Control Division
Automatic Control Research Group
Chalmers University of Technology
Gothenburg, Sweden 2022

Optimal control of reconfigurable multi-battery systems
NAUMAN KHURSHID HAIDER

Supervisor: Faisal Altaf, Electromobility Department, Volvo Group, Gothenburg, Sweden
Examiner: Changfu Zou, Department of Electrical Engineering, Chalmers University of Technology, Gothenburg, Sweden

Master's Thesis 2022
Department of Electrical Engineering
Systems and Control Division
Automatic Control Research Group
Chalmers University of Technology
SE-412 96 Gothenburg
Telephone +46 31 772 1000

Cover: Overview of a electrical drive system in a typical Electric Vehicle. Modification of a demo simulation pertaining to vehicle control in AMESIM software.

Typeset in LaTeX
Printed by Chalmers Reproservice
Gothenburg, Sweden 2022

Optimal control of reconfigurable multi-battery systems
NAUMAN KHURSHID HAIDER
Department of Electrical Engineering
Chalmers University of Technology

Abstract

In the last two decades automotive sector has been working towards electrification in a bid to replace fossil fuel vehicles and reduce green house gases emissions. Most of the companies until recently have focused the efforts towards small passenger vehicles as heavy vehicles have greater power demands and far more complex control requirements as trucks spend on average 14 hours per day on the road compared to passenger vehicles that are parked 95% of the time [1]. However the advancements in battery manufacturing techniques and control methods has brought forward solutions that have made it possible to bring electrification in heavy vehicles and marine applications. Due to high power demands, the vehicle vehicles require more than one than one battery pack in its energy storage system (ESS). These batteries are connected in series and/or parallel configuration in order to fulfill the load requirements. This makes the control problem unique and more challenging compared to passenger vehicles using single battery pack.
Balancing load among all the battery packs in the ESS is of utmost importance to achieve optimal performance and increase through put of the system. In this thesis, optimal control of reconfigurable battery system (RBS) is investigated for application in battery-powered electrified vehicles (xEVs). The RBS through optimal switching enables distribution of load among various packs in an optimal way to increase systems power capabilities. The optimal control problem is formulated for load sharing with the main objective of maximizing state-of-power (SoP), charge and thermal balancing observing given physical constraints (dynamics, safety, health, power limits etc.) of each unit. The control problem is then solved in a receding horizon fashion using a model predictive control framework. A comparison between the proposed control framework with that of conventional (fixed) multi-battery system using different load cycles and operating conditions. The results illustrate that power capacity of ESS can be increased with an RBS system compared to a conventional battery system.

Keywords: Reconfigurable Battery System, Charge Balance, Thermal Balance, Optimal control, Battery Management System, Model Predictive Control, Battery Load Sharing, State of Change (SoC)

Acknowledgements

First of all, I am highly grateful to Allah Almighty for His blessings that made it all possible.
I would like express heartfelt gratitude to my thesis supervisor Faisal Altaf, Chief Engineer / Chief Architect, Electromobility Department, Volvo Group Trucks Technology for his utmost guidance, continuous support and valuable feedback. He provided me with data required for carrying out the work. His support was exteremly valuable in decision that shaped the outcome of this thesis. I am also grateful my examiner Prof. Changfu Zou for his invaluable guidance and constructive feedback thorough out the process that helped in completing the thesis. I would also like to thank Yang Xu (Volvo Group), Prof. Torsten Wik (Chalmers) and Albert Skegro (Chalmers) for their time and helpful feedback on the report.
I would like to thank all sincere friends for their support and encouragment through out the process.
In the end, I am extremely beholden to my family for their unending love and unconditional support through out my life .

Nauman Khurshid Haider, Gothenburg, June 2021

Contents

List of Figures

List of Tables

1
Introduction

A brief introduction to the report is presented in this chapter that is divided into four sections. First section 1.1 discuses the background of the thesis work and presents literature review on the topic. Section 1.2 presents a conventional battery system while a reconfigurable battery system is defined in section 1.3. In the final section 1.4 problem is defined along with thesis objectives, methods used and circumscription associated with this thesis work.

1.1 Motivation

Demand for sustainable power alternative is on the rise driven by the depleting natural resources (fossil fuels), negative impact of increasing carbon footprint, and need to address the pressing issue of global warming. Automotive sector is playing lead role in offering substitute for vehicles with low fuel efficiency in the form of fully or hybrid electric vehicles. This change has also been necessitated by United Nations through sustainability goals set for year 2030 in the Sustainable Development Summit 2015 [8] as well as the 2015 Climate Change Paris Agreement [9]. EU under its wider climate and energy framework 2030 has set target to reduce emissions by 55% by year 2030 from the levels of 1990 [10]. Many automotive companies are researching for the alternates and replacing fossil fuel powered internal combustion engines (ICEs) with hydrogen powered ICEs, bio-gas solutions or fully electrified vehicles powered by batteries.
Electrified vehicles hold major share among these alternatives and significant research is ongoing to find reliable and efficient energy storage system (ESS) that is cost effective as well. Lithium ion batteries (LiBs) are preferred choice for ESS due to their superior cyclic performance and comparatively high power capacity opposed to other available systems [11]. ESS in an electric vehicle comprise of several battery packs/ cells connected in series and/or parallel configuration to obtain desired power output. Also LiBs are highly sensitive to operating conditions and require special handling to maximize battery life and power capabilities. Due to these factors there is a need for a battery management system that can couple all these power units to deliver desired output in a most efficient manner. Managing several cells/ packs operating together becomes specially challenging given the parametric variations of one unit from the other. These parametric variations (internal cell parameters like resistance and charge capacity) are due to inevitable manufacturing tolerances even in cells from a same batch [12]. These parametric variations increase further with usage as the battery ages with various factors such as State of Charge (SoC), c-rate,

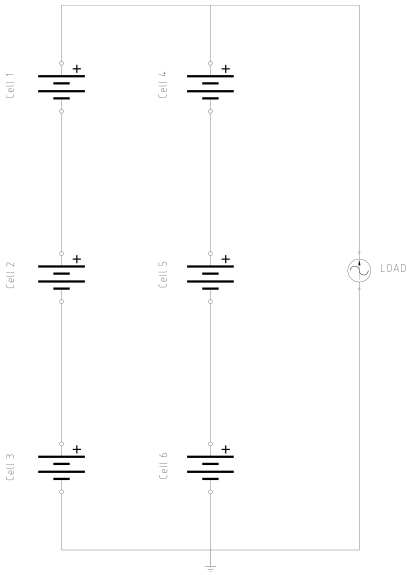

Figure 1.1: Conventional Battery System with bi-directional current source as load

operating temperature, and depth of discharge (DoD) greatly affecting it. Typically a cell will age rapidly under high temperature, SoC and DoD compared to the one exposed to lower magnitudes [13, 14, 15, 16].

1.2 Conventional Battery System

Figure 1.1 shows a conventional battery system (CBS) where cells are assembled in a fix configuration in series, parallel or combination. With this configuration the system power capabilities are limited by the weakest cell in the system as we cannot control flow of power through each individual cell so a cell with lowest current carrying ability will create a hard constraint (i.e., so-called weakest link in the chain) for the whole pack. During the charging phase, charging will stop as soon as the weakest cell reaches full capacity, similarly the discharge will come to halt once the weakest cell has drained to lowest energy level. Another drawback of this configuration is if any cell fails or malfunctions the whole pack becomes incapable to provide power thus rendering all the healthy cells useless despite only a single faulty cell. In order to get maximum power capabilities all the cells in a conventional battery pack must be identical to each other. Also building a pack from all cells with identical power capabilities is practically hard due to inevitable parametric variations even at beginning of life. Usually, during the assembly process, the cells are sorted according to their capacity (and possibly resistance) values. Some strategies prefer placing similar cells in modules. Some other strategies prefer placing cells in modules in such a way that the performance across the modules is equalized. Despite this characteristics of cells will vary almost inevitably over operational life due to non-uniform aging in conventional battery systems.

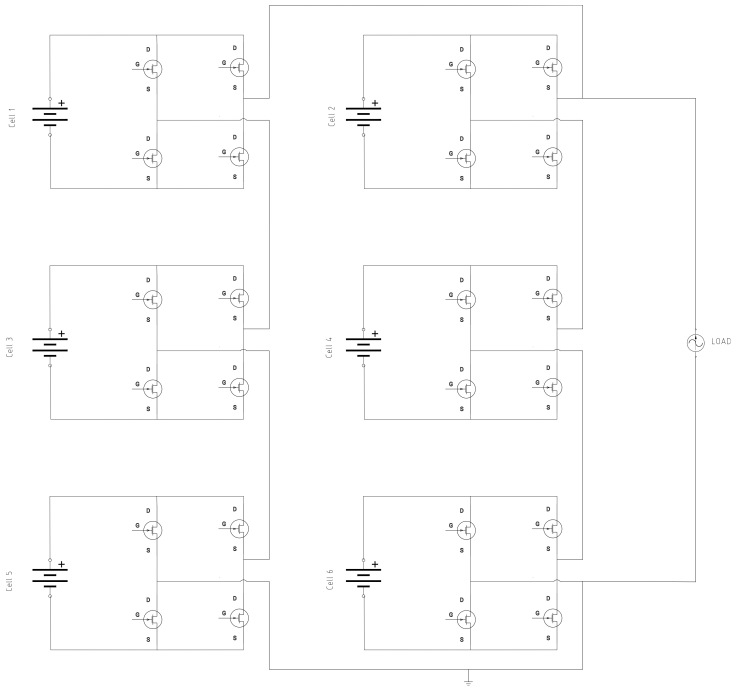

Figure 1.2: Reconfigurable Battery System with bi-directional current source as load

1.3 Reconfigurable Battery System

Figure 1.2 depicts a reconfigurable battery system (RBS) where connection topology can be manipulated at a cell, module and/or pack level as desired. Some brief benefits of RBS are listed as below:

- **Enhanced Fault Tolerance:** Any faults in the cell be it internal or external (such as short circuit) may affect/ damage the cell while also affecting the neighbouring cells. This might affect the whole system to the point where it becomes incapable of delivering power at all thus escalating a small fault at cell level to the entire pack. It can also lead to greater safety risks such as fire and explosion, a catastrophic outcome putting both user and the device at risk. Such risk can be avoided with the help of RBS where faulty cell can be immediately isolated from the system while keeping remaining cells connected without disrupting the operation [17, 18, 19, 20]. An example of fault isolation can be seen in figure 1.3(a) where malfunctioning cell (C_2) has been isolated while keeping the remaining healthy cells connected and in operation.
- **Charge and Thermal Balancing:** No two cells are identical in a pack due to manufacturing tolerance within same batch, assembly variance arising from cells of different batches used together, impurities, aging and environment they are exposed to results in heterogeneities. Imbalance in charge will reduce the system power capabilities thus some of the cells will be underutilized while others overutilized. This also leads to premature degradation of the system [21] and other safety issues [22]. Thermal imbalance result in each cell aging at a different rate whilst also reducing the battery life and has significant impact

on power ability of battery system. System might also experience issues of overheating which is a major safety concern and fire hazard. The CBS' use additional balancing circuits and cooling devices to address these issues with a BMS [23, 24, 25]. However, in a RBS this can be achieved with intelligent reconfiguration of the system. Figure 1.3(b) illustrates how through system reconfiguration cell balancing is achieved in roughly half the time compared to conventional system [2]. Similarly thermal balancing can be achieved by intelligently handling cell current [26, 25, 27, 28, 29, 30, 31, 32].

- **Extended Power ability:** Faster and increased power conversion during both discharge and charge cycles can be achieved with smart scheduling of battery operation. For example, if during a charging phase if a cell reaches a set higher threshold it can be disconnected and rested while remaining cells continue to charge. By this way all the cells can be charged to same threshold without compromising the system's chargeable power ability. Same principle applies in case of discharge cycle where once a cell is drained to a lower set point it can be removed from cell string. Illustration of this can be seen in figure 1.3(c) here lines c and d represent the charging and discharging current lines. It was shown in [33, 34] that total energy output of a system can be increased substantially by such scheduling of battery operation.
- **Synchronizing Different Batteries:** Manufacturing variance among battery cells coupled with operational conditions means that battery cells are continuously aging resulting in increase of internal ohmic resistance and decrease in charge capacity. This makes battery management problem for batteries with different ages even more complicated. In general practice, battery cells with capacity less than 80% of the initial are deemed unsuitable for EV applications and are replaced [35]. These batteries however still can be used as stationary energy storage such as power grids with less demand in terms of energy density and less intense operating condition [36]. RBS in this case plays an important role for second-life applications besides extending the first-life usage. Figure 1.3(d) depicts this cycle pertaining to second-life usage of EV batteries.

  Similarly batteries of different chemistry can be synchronized using similar technology *software defined batteries* (SDBs) proposed in [37] as depicted in 1.3(e). The objective here is to combine strengths of batteries of different chemistry via dynamic reconfiguration as different commercial batteries perform differently in various applications with some better suited than others.
- **Customized Output Range:** Compared to CBS with fixed terminal output, the output of a RBS can be customized to the requirement. EVs require several converters to supply power to all the components with different power requirements. This requirement of added equipment can be circumvented through RBS which is fully capable of delivering power to various loads with wide range of operating voltages. Figure 1.3(f) displays power requirements of various components in a medium passenger size EV.

1.4 Thesis Objective, Scope and Outline

This thesis is summarised as under:
Chapter 1:
It introduces the thesis topic along with the objectives set for the thesis and contributions in terms of scope.
Chapter 2:
In Chapter 2, a brief overview of Li-ion batteries is presented for readers that are less familiar with the cell chemistry and operations of it. It also discusses the terminologies used throughout the thesis.
Chapter 3:
Here battery management system is presented for readers that are less familiar with the topic along with its features, topologies, some balancing techniques and their comparison.
Chapter 4 and 5:
System Architecture is presented in chapter 4 while state space model is defined in chapter 5 for the model used during the investigation of this thesis work.
Chapter 6:
Control scheme for the MPC framework together with the objective function and necessary constraints are defined in this chapter.
Chapter 7:
Results for the defined control scheme using various operating scenarios are presented in this chapter.
Chapter 8:
The results are discussed here and main findings are summarized. Contributions made by this work are also presented here along with possible future work directions.

1.4.1 Objectives

The objective of this thesis work is to investigate following:

1 **Modelling the RBS state-space:**
   a. How can the RBS be modelled such that the model is both computationally efficient and simple to parameterize?
   b. Can the obtained model be made generic so that it is scalable and configurable for any number and types of batteries?

2 **Load sharing problem formulation as optimal control problem:**
   a. Formulate the optimal control problem for load sharing with the main objective of maximizing state-of-power (SoP) based on the model developed in Step 1 while respecting given physical constraints (dynamics, safety, health, power limits etc.) of each unit.
   b. Solve the optimal control problem in the receding horizon fashion using a model predictive control framework.

3 **Analysis and verification of the proposed control framework:**
   a. Compare the proposed control framework with the one used for conventional (fixed) multi-battery system using different load cycles and operating conditions.

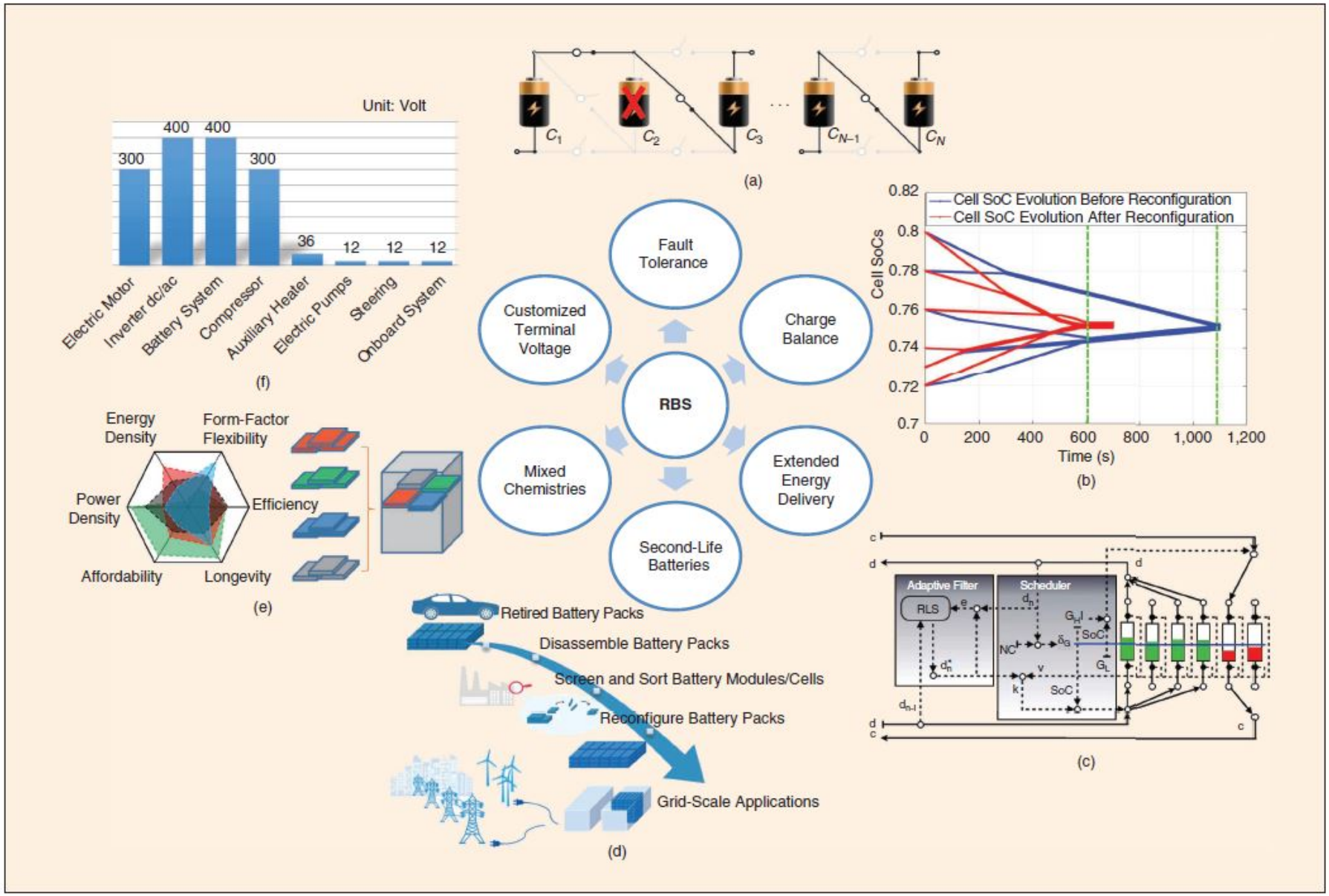

Figure 1.3: (a) Fault isolation, (b) Accelerated charge equalization, (c) Scheduling network, (d) Second-life usage, (e) Different battery chemistry, (f) Voltage requirement of different EV components in medium passenger size EVs [2]

b. Evaluate the potential benefits associated with operation of reconfigurable energy storage systems (RESS) using advanced controls found using MPC framework.

1.4.2 Method

The approach for solving research questions in section 1.4.1 is as follows:

1 **Modelling the RBS state-space:** The control-oriented model is a scalable state-space representation of RBS for any configuration (i.e., connection topology) and type of cells. It is developed based on equivalent-circuit model (ECM) approach where the fast switching behavior is modeled using circuit averaging techniques [2, 25, 38, 39].

2 **Load sharing problem formulation as optimal control problem:** Use MPC RHC techniques to find the optimal control strategy for the proposed control-oriented system model with objective of maximizing power ability (SoP) of the system while respecting the constraints related to system dynamics, safety, health, power limits etc. of each battery unit. [25, 26]

3 **Analysis and verification of optimal control scheme:** Verify the performance of the proposed control framework using various test scenarios covering experimentation using battery packs with varying level of heterogeneity among the cells within the pack under different system constraints.

4 **Experimentation with constraints:** Initially, for the development of the control strategy hard constraints on power required will be imposed. This however, will be changed afterwards by introducing some slackness in order to evaluate control feasibility when 100% power cannot be delivered for longer period of time. This part involving optimal solution when requested power can't be fully delivered presents additional research objective.

1.4.3 Main Limitations and Assumptions

The limits considered for this thesis work are stated as follows:

1 **Control Freedom:**
A limit on control freedom for this thesis consists in active control not being allowed for all battery packs. Active control is implemented for one battery module in the pack at a time, while the control for the remaining battery pack is simulated via average switching. $\Delta u = 0$ leads to infeasible solution as the control scheme is aimed towards faster balancing while continuous switching between +ve and -ve currents in load cycle and varying magnitude makes it harder to get a feasible solution with delta $\Delta u = 0$ for rest of the cells.

2 **Data:**
Data subjected to *General Data Protection Regulation (GDPR)* is provided by Volvo Group. Research carried out is based only on this data.

3 **Model Fidelity:**
As mentioned in section 1.4.1, two models are being investigated in this thesis. However, their level of fidelity is different.

a. **Plant model**: High-Fidelity with focus on simulating system performance close to reality.

b. **Control model**: Low-Fidelity setup within which several parameters are assumed constant if their impact on system performance is deemed insignificant. This is done to reduce the computational complexity of the model.

4 **Uni-polar switch model:**
Uni-polar switch model configuration (using DC-DC converter) is considered within the scope of this thesis [31]. This means that all modules are being either charged or discharged at any time instant, which simply means that any two or more cells/modules in a string are not allowed to have opposite polarities i.e., we do not allow charging of some cells while discharging others or vice versa.

2

Overview of Lithium-Ion Batteries

In this chapter some basics related to battery are discussed for readers who are less familiar with the subject, well versed readers can skip this chapter. In the first section 2.1 battery construction are discussed while the second section 2.2 deals with different configurations used in common battery applications. The final section 2.3 is dedicated to definition of some common battery terminologies that is frequently used in this work.

2.1 Construction and Chemistry

Lithium-Ion batteries (LiBs) being a popular choice nowadays as portable and rechargeable source of electrical power were first commercially developed and introduced by Sony Group Corporation and Asahi Kasei Corporation in 1991 [40]. Since its introduction LiBs have significantly replaced other battery types such as Lead acid, Ni-Cd, Zn-MNO_2 due to its superior energy density, power density, and cycle life. The LiB also consists of a positive electrode and a negative electrode submerged in an electrolyte solution and separated with a film (i.e., separator) that only permits the flow of lithium ions through it. This separator is crucial for safe operation of the battery as it precludes contact between anode and cathode [41].

In the charging phase, oxidation reaction[1] occurs on positive electrode where the electrons move from positive electrode to negative electrode through the external circuit while the Li-ions move from the positive electrode internally through the separator to negative electrode, where reduction reaction[2] happens (i.e., internally displaced lithium ions get neutralized by gaining externally displaced electrons).

During discharging lithium ions move in opposite direction i.e., from negative electrode to positive electrode (oxidation happens on negative electrode and reduction happens on positive electrode).

The definition of anode is electrode where oxidation occurs and cathode where reduction happens. Thus during charging positive electrode acts as anode whereas negative electrode acts as cathode. Similarly during discharging positive electrode acts as cathode whereas negative electrode acts as anode. The charge and discharge

[1] Oxidation: Loss of electron in an ion or atom
[2] Reduction: Gain of electron in an ion or atom

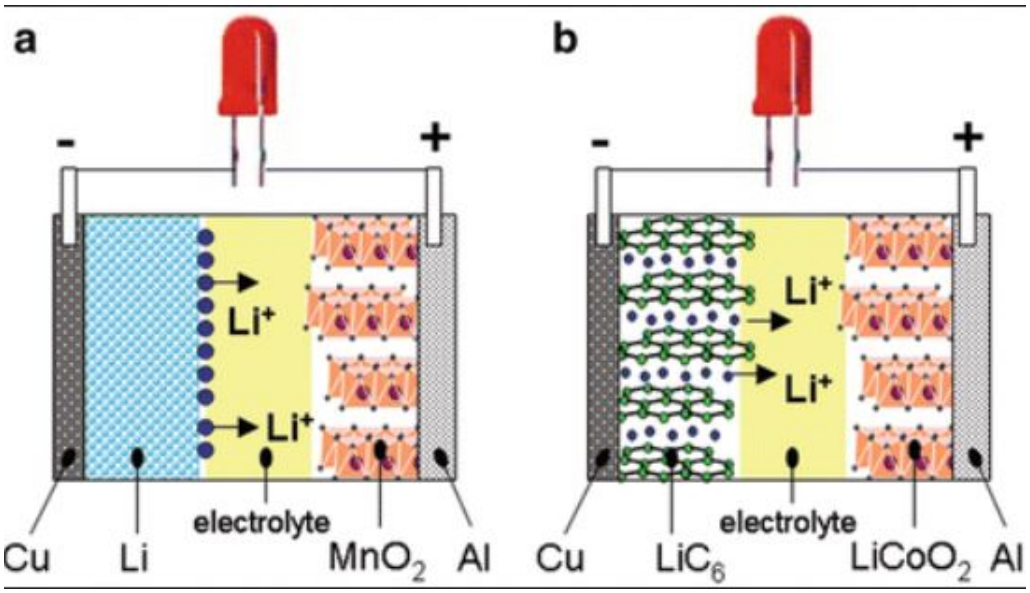

Figure 2.1: Structure of a Lithium-Ion Battery showing electrodes and electrolyte. In (a) negative electrode is formed with pure Li while (b) uses a Li-insertion compound (graphite) [3]

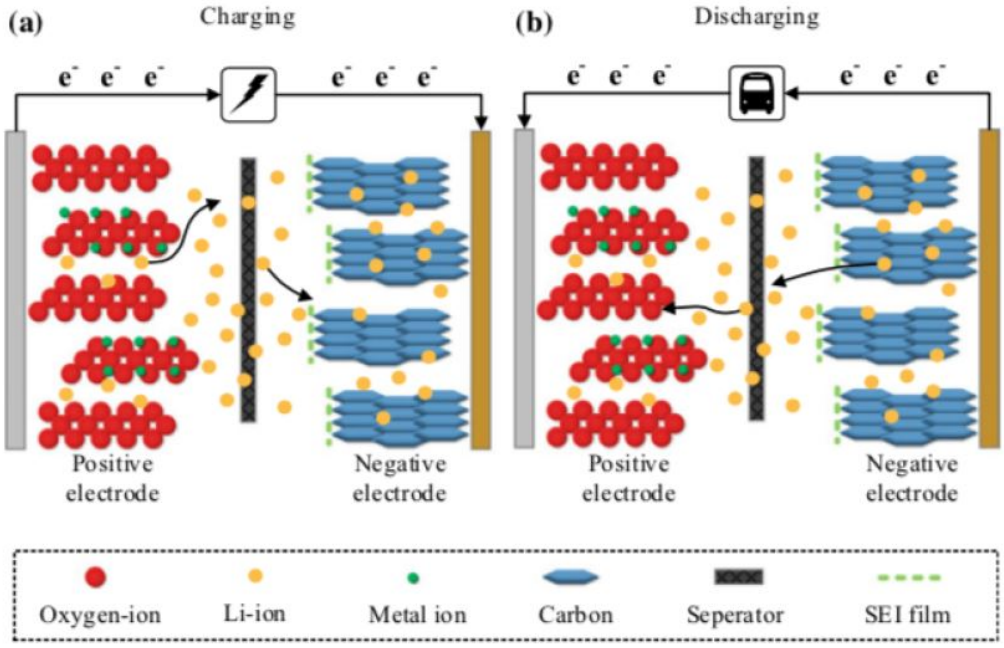

Figure 2.2: Charge and discharge processes inside a LiB [4]

processes are shown in figure 2.2 [42, 4].

2.2 Connectivity

The smallest unit in a battery is a cell which have two types depending on its rechargability. Primary cells are the one time use cell and cannot be recharged while secondary cells can be recharged multiple times over its life-cycle.
Two or more cells are connected in series and/or parallel to form a battery module depending upon the application and power requirements. When cells are connected in series the capacity of the pack is the same as the cells but output voltage increases and thus energy and power ability increases. In case of parallel connected cells the overall voltage is same but capacity increases [7] shown in figure 2.3. Several battery modules are then connected together to form a battery pack. The difference between two is the individual adoption for a certain application. Table 2.1 enlists the various applications as per the power requirements.

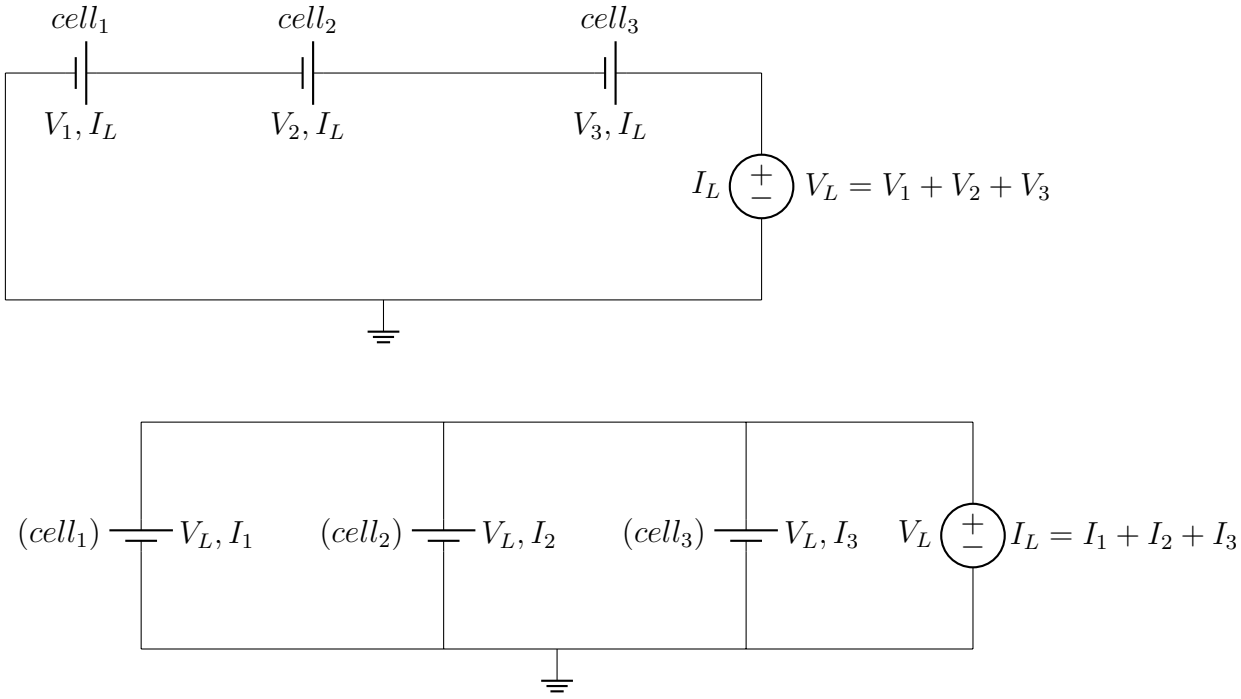

Figure 2.3: Series and Parallel configuration

Application	**Power Requirements (Wh)**	*SystemRequirements*
Smartphone	5	Energy Density
Laptop	50-100	Energy Density
HEV	1000	Power and lifetime
PHEV	5000-10000	Energy Density and Power
BEV	15000-50000	Energy Density
Power/ Grid station	5000-10000	Power and lifetime

Table 2.1: Battery Applications and power requirements [7]

2.3 Terminologies

Some common battery terminologies pertinent to this thesis are briefly presented here.

- **Cell Capacity (Q) [Ah]:** Cell capacity also known as total charge capacity is the amount of charge that a cell can store. It is represented in Ampere-hours (Ah) or milliAmpere-hours (mAh) for smaller capacity cells used in less power demanding applications.
- **C-rate:** It is the rate at which a cell is discharged in light of its maximum capacity. For example 1C-rate for a battery cell with maximum capacity of 1 Ah will be 1 A. Similarly 10C-rate will be 10 A.

$$C - rate = \frac{\text{Battery Current}}{\text{Nominal current}} \tag{2.1}$$

- **State of Charge (SoC) [%]:** It is the ratio of battery's dis-chargeable capacity in its current state to its maximum dis-chargeable capacity at its fully charged state. It is represented as a percentage and ranges from 0-100%. This is represented as ξ in this thesis work.

$$\xi = \frac{\text{Current capacity}}{\text{Max dis-chargeable capacity}} \times 100\% \tag{2.2}$$

- **State of Health (SoH):** It is the criterion to assess the current maximum of battery in light of its rated capacity (newly manufactured cell). For example SoH of a new battery will be 100% since it matches the specifications and will degrade over period of usage.

$$SOH = \frac{Q_{max}}{Q_{rated}} \tag{2.3}$$

- **Depth of Discharge (DoD):** It is the percentage of battery capacity that has been discharged relative to its maximum capacity. Generally a deep discharge means 80% DoD.
- **Open Circuit Voltage (OCV):** Open circuit voltage is the voltage across cell terminals when no load is connected to it and no external current flows between them. It is function of SoC and temperature.
- **Terminal Voltage (V_B):** This is the voltage of a cell/ pack when load is connected to it. Relationship to find terminal voltage is shown in eq. (5.6) in Chapter 5.
- **Polarization Voltage (PV) [V]:** It is the measure of voltage loss in a battery when current passes through it. It can be calculated from eq. (5.6) in Chapter 5 where V_0 and V_1 represents polarization voltage. It is the difference between OCV and V_B [43].
- **Internal Resistance (R_s):** All the batteries have internal resistance due to elements such as electrolytes and electrodes not being ideal conductors. Voltage drop occurs across these elements due to their resistivity. Internal

resistance of battery cell is a function of SoC and temperature. It is also affected by state of health (SoH) of battery and increases with age. It is combination of ohmic resistance and dynamic resistance (modelled by RC elements).

- **Energy Density [Wh/L]:** It is the ratio of nominal battery energy to unit volume.
- **Max. Continuous Charge/ Discharge Rate:** This is the rate of continuous charge/ discharge specified by manufacturer in order extend useful life of battery and preclude any damage to it from extreme operating conditions.
- **End of Life (EoL):** Typically when the battery SoH has degraded to 80%, the battery is said to have reached its End of Life however it generally depends on vehicle energy and power requirements. For EV applications this is the point when the battery is taken out of service and replaced [44].
- **Cycle Life:** Cycle life of a battery expresses how many times a battery can be fully charged and discharge before EoL. One cycle is one complete charge and discharge.
- **Coulomb Efficiency (η):** It is the ratio of discharge to charge capacity and is a metric for evaluating battery efficiency [45].

$$\eta = \frac{Q_{discharge}}{Q_{charge}} \tag{2.4}$$

- **Energy Efficiency:** It is the ratio of energy out to energy in i.e., ratio of total energy delivered (from battery terminals) during discharge from 100% to 0% SoC and energy received (from charger to battery terminals) during charge process from 0% to 100% SoC.

$$EE = \frac{\text{Energy out}}{\text{Energy in}} \tag{2.5}$$

This is also expressed as the multiplication of Coulomb efficiency and voltage efficiency [45].

3

Battery Management System

A brief introduction to battery management system (BMS) is presented in first section 3.1. Section 3.2 discusses some interesting features of a BMS while some common topologies in literature are shown in section 3.3. Use of BMS to achieve system balancing are discussed in the final section 3.4.

3.1 Introduction

A BMS is used to ensure safe operating conditions of a battery, optimize its usage, extend life, and estimate its states. It makes usage of battery reliable, cost effective and safe in applications. In an EV application the safety is a major concern for battery packs especially protecting the occupants from hazards such as fire and shock etc. Continuous monitoring of battery states specifically during charging and discharging is critically important. Also thermal management to ensure battery always operates within safe operating temperatures to prevent any failures and increase the power efficiency. Some applications of BMS involve electronic circuitry geared towards protection against high and low voltages [46] while others are more profound and provide accurate battery management by monitoring states such as SoC, SoH, etc along with temperature, current and voltage through each cell [5]. They also use sophisticated algorithms to compute remaining useful life (RuL) of battery and protect a battery from operating in hazardous and unsafe operating conditions. Charge and thermal balancing is also achieved with the help of a BMS which ultimately results in extended useful life and maximising the power capability of whole system.

Figure 3.1 shows the overview of a BMS. It can be seen that it consists of sensors that provide data of measurable states such as current, voltage and temperature of each cell as inputs. A state estimator is then used to compute unmeasurable states such as SoC, SoH, diffusion voltages etc which are cardinal for optimizing performance of battery. The control algorithm makes use of the states data along with power requirement from user of present time to compute and deliver to deliver required power using the electrical control unit. A safety protection unit monitors the operating conditions and kicks in to isolate the battery if any safety is breached to prevent catastrophic failures. Similarly thermal management unit ensures the battery is always operating with recommended safe working temperatures to enhance the output efficiency.

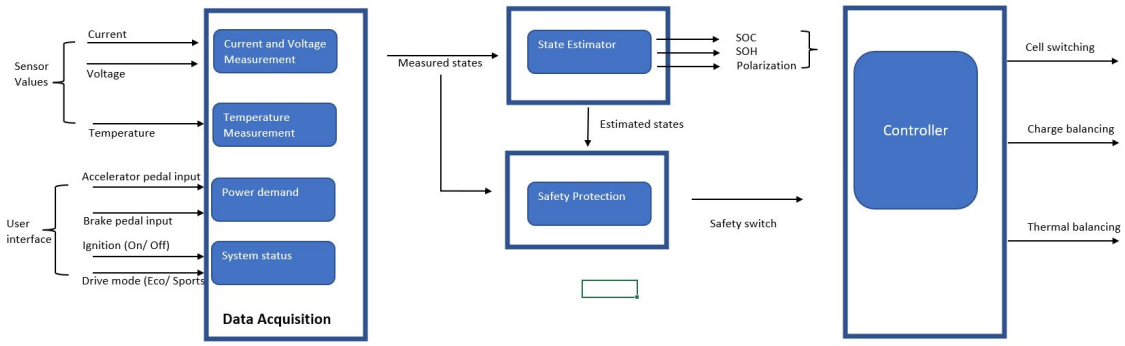

Figure 3.1: A generalized overview of BMS

3.2 Features

In order to ensure smooth operation within recommended safety margins while meeting power demands in a manner that maximizes the power capability of the system a BMS needs to have following features:

- **Cell Monitoring:** The objective of cell monitoring is the data acquisition. Voltage, current and temperature measurements from sensors are obtained here to be used for estimation of unmeasureable states and other applications.
- **Safety Protection:** Safe working of the system is ensured via this feature. The operating conditions of the battery are continuously monitored and any hazardous conditions arising from battery chemistry or use beyond permissible limits are prevented. The safety protection covers scenarios such as over-charge, over-discharge, over-current protection/ short circuit, thermal run-away, etc.
- **SoC Estimation:** SOC is a measure of charge capability of a battery, it represents how much charge is available as compared to its maximum charge capacity. It is paramount for the optimal energy management and also good way of preventing overcharge and discharge scenarios. Since the SOC cannot be directly measured, it has to be estimated using algorithms based on experimentally gather data.
- **SoH Estimation:** SoH is a life-guage of battery i.e., it indicates level of energy and/or power fading that has happened so far. Based on SoH and usage historical data, remaining-useful-life (RUL) of battery can be predicted, which is useful for predictive maintenance services (i.e., to predict in advance when battery replacement will be needed). It is a good criterion of battery functionality and control action be selected based on it to ensure optimal usage that extends useful life and power capabilities of the pack. Just like SoC, SoH too has to be estimated as it cannot be measured directly.
- **Cell Balancing:** In EV and grid applications several cells are connected with each other to form a battery pack. A battery pack is as strong as its weakest cell. In a battery no two cells are ever identical, even cells of same batch vary from each other slightly due to manufacturing tolerances. Even if the cells were somehow identical in the beginning they will tend to diverge over the

lifetime due to slight difference in operating conditions. This variability in operating conditions and environment is inevitable and cannot be prevented completely. It directly affects the internal resistance, charge capacity of the cell. Through cell balancing techniques these variations can be minimized and useful life of whole pack can be extended significantly [13, 14, 15, 16]. The balancing techniques will be discussed in detail in this chapter later on.

- **Thermal Management:** Thermal management has two goals to achieve: (i) Ensure operating temperature is within safe limits for optimal performance e.g., typically operating range of LiBs is (25^o-35^oC), and (ii) To reduce thermal imbalance between cells. Just like SOC imbalance, thermal imbalance occurs in cells due to manufacturing tolerances, variations in internal resistance and coolant temperature gradient. These variations are often not negligible in EV and smart grid applications [13, 14, 15, 16] and must be taken in to enhance power capabilities of the system since the whole pack can reach EoL earlier because of premature failure of any one cell. The balancing techniques will be discussed in detail in this chapter later on.
- **Charge/ Discharge control:** The control algorithm is used to compute input of switching for each cell in a manner to achieve SOC and thermal balancing along-with maximal power capability of the whole system. Same is responsible for protecting individual cell from exposure to overcharge/discharge and isolate it from system in case of failure to keep rest of the system operational.

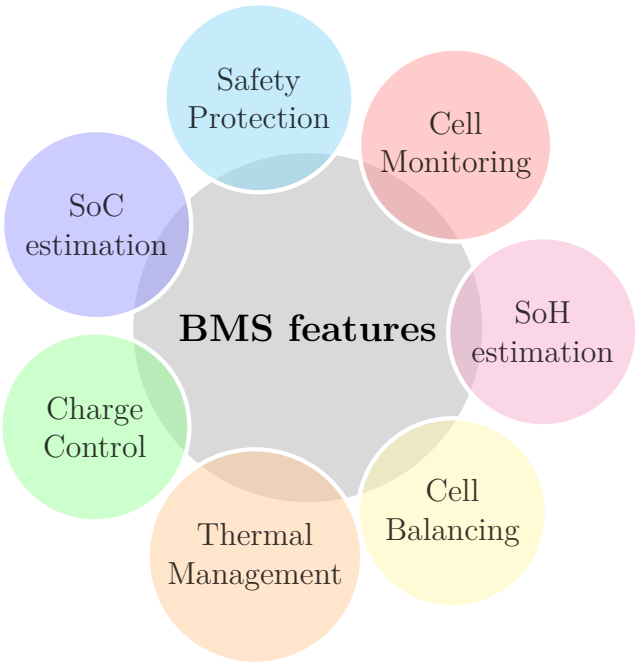

Figure 3.2: Features of BMS. Modification of flowchart in [5]

3.3 Topologies

In terms of topology, BMS can be categorized into three classes:

- **Centralized:** In the centralized BMS a single control is used and is connected to all the cells within the system. This sort of arrangement although is simpler to implement but is often messy because of several wires running increasing chances of mistake. One more pitfall is that complete system depends on one BMS module.
- **Distributed:** In a distributed BMS, each cell is controlled by individual BMS and a single communication cable connects battery to the controller. This setup although increases hardware cost but it is more robust since performance of complete system doesn't hinge on a single BMS system. They are simpler to install and offer clean assembly.
- **Modular (Semi-distributed):** Whole battery pack is divided into different modules comprising few cells each controlled by a single controller. All the controllers are connected with each other. This type of BMS is a compromise between the centralized and distributed controllers.

3.4 Balancing

One of the important tasks of BMS is balancing of cells in terms of SOC and thermal properties. Since no two cells are identical in a pack due to manufacturing tolerance within same batch, assembly variance arising from cells of different batches used together, impurities, aging and environment they are exposed to results in heterogeneities. Service life and capacity of a battery pack can be maximized via cell balancing over SOC. Balancing is solely required when there are two or more cells connected in series and not necessary for cells in parallel since cells in parallel configuration will balance each other automatically.

3.4.1 Balancing Techniques

Cell balancing has two main topologies discussed below. A brief overview of them is shown in figure 3.3:

3.4.1.1 Passive (Dissipative)

Passive balancing is straightforward and easiest to implement. The setup consists of a control switch and a fixed or switching resistor connected with each cell. Cells with higher energy are drained and excess energy is dissipated as heat to match the energy of the lowest cell in the pack. The disadvantage of this technique is that excess energy is just wasted away and dissipation as heat also intensify the thermal balancing. Another issue is that in order to avoid overheating problem the balancing current is limited thus it requires long balancing time [47]. This also limits the total power capacity of whole pack to that of lowest energy cell[48].

3.4.1.2 Active (Non-Dissipative)

Active balancing methods use capacitors, inductors or DC-DC converters to equalize the energy of all cells in the battery pack. In this technique, energy is transferred from higher cell to lower cell instead of being dissipated as heat. It can be employed for all cell types regardless of chemistry. It has high efficiency and balancing speed however the cost is higher compared to passive method. It is further classified to three types based on the active element used for balancing:

Transformer/Inductor based: In this setup inductor or transformer is used to move energy from one cell to another in the pack. Cell balancing can be achieved quickly however high cost of transformer along-with requirement of filter capacitor makes it expensive of the methods. Several variations such as Single winding and multiple winding transformers and inductors exist [49, 50].

Capacitor based: Capacitors are used here to shift energy from one cell to another in the pack. This technique has a drawback of slow balancing charge and high losses [51].

Converter based: Converter based balancing approaches are gaining traction in recent years as it provide great control freedom over whole balancing process. Major issue in this technique is high complexity of the system and expensive hardware setup required to achieve objective. Technological innovations have given rise to several variations for this technique as shown in graph 3.3. This thesis work makes use of DC-DC converters to achieve balancing among the cells of the system.

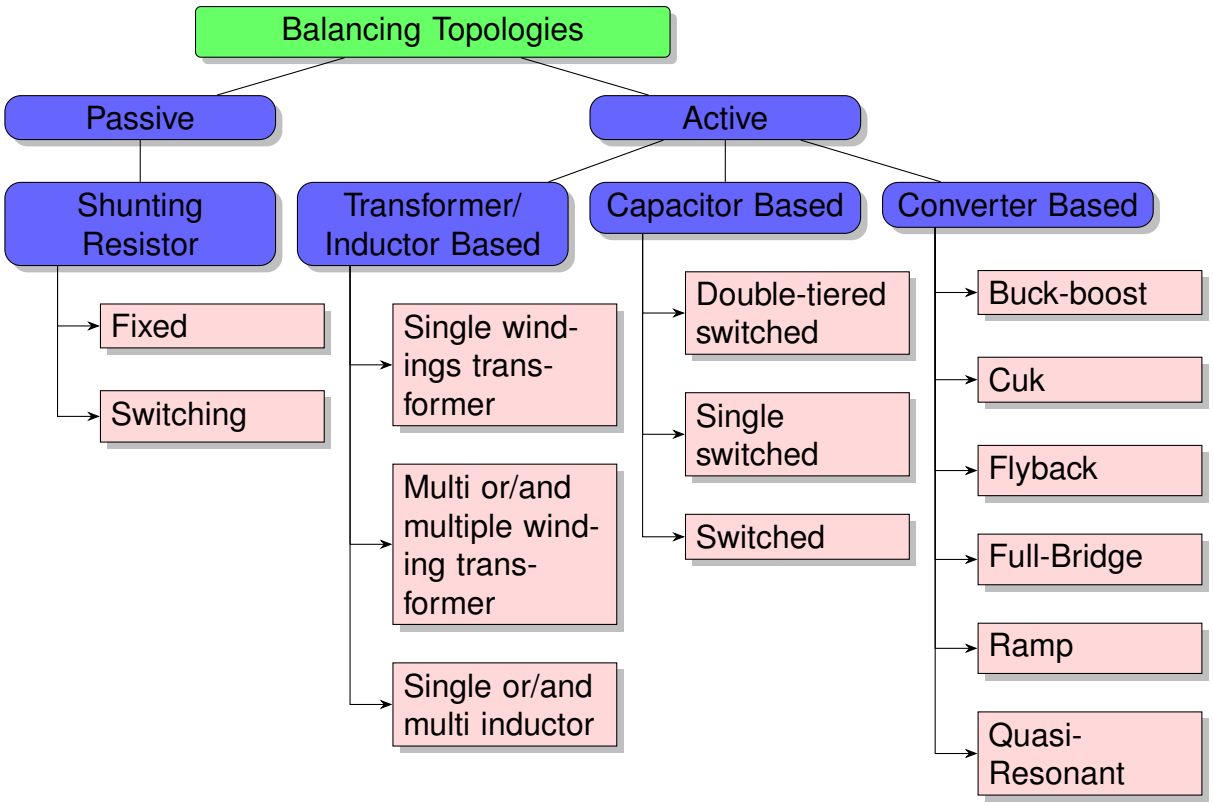

Figure 3.3: Cell Balancing Topologies [6]

3.4.2 Comparison:

As can be seen in figure 3.4 there are three cells in a pack A, B, and C with initial SOC values 85%, 75% and 65%. If no balancing is applied the maximum pack capacity will be limited to the lowest value cell i.e., 65%. Over the operation the weakest cell C will experience accelerated aging and deterioration of the cell due to to different SoC swings and due to over-charging or over-discharging of the cell C thus further increasing the variance. With passive balancing the energy from cell A and B will be dissipated in the form of heat and brought down to the level of the weakest cell C. In this case the maximum capacity of the whole pack will still be 65% but since all the cells are balanced thus no one cell will be stressed during operation thus aging of cells will be uniform. In the active balancing the charge from cell A will be transferred to cell C thus the capacity of entire pack will now be equal to average of all the cells which in this case will be 75%. This clearly shows that almost 10% of the pack capacity was either unused (in case of no balancing) or wasted (in case of passive balancing). Thus by active balancing technique not only the power capabilities of pack are increased but also operational life will increase as well [52].

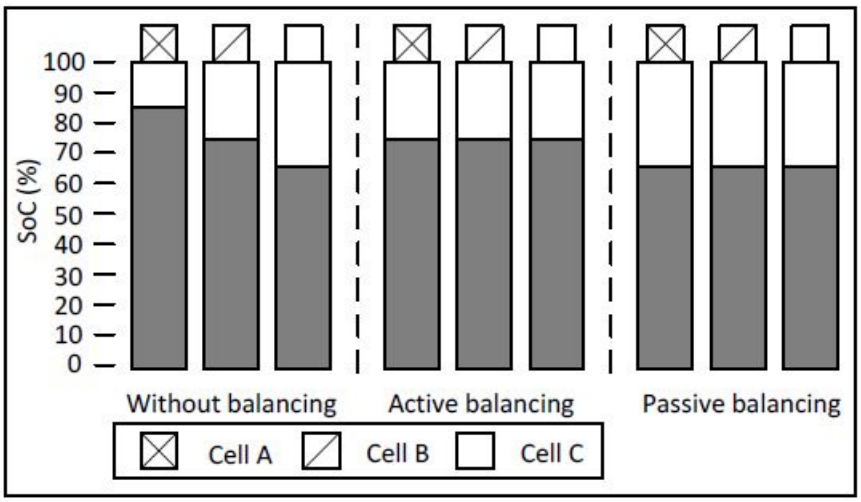

Figure 3.4: Comparison of balancing methods [6]

4
System Architecture

This chapter presents the switching characteristic that will be part of system model to be used. The first section 4.1 presents switching function, the average switching relation and modular pack architecture with multiple battery cells/modules connected in series. Section 4.2 discusses the control operation using switches while section 4.3 shows relation between cells terminal properties and the connected switch.

4.1 Single Pack Architecture

The reconfigurable battery system comprises n-power units (PU) connected in series to form one battery pack shown in figure (4.2). These PU:s may consist of either individual cells or smaller battery modules/packs connected in series. Inside each PU there is a power source (individual cell/ battery pack) connected in series with a H-bridge/ Full bridge (FB) circuit shown in figure 4.1. The H-bridge is used to simulate average switching and it also isolates the cell from rest of the circuitry. Each PU has terminal voltage $V_{Li}(t)$ supplied to a variable load with load current $i_L(t)$. All the PUs in series together provide the total load voltage $V_L = \sum_{i=1}^{n} V_{Li} \in [0, V_{L,max}]$ where $V_{Li} \in \{-V_{B_i}, 0, +V_{B_i}\}$ and V_{B_i} being the terminal voltage of individual cell. Each FB has switching function $s_i(t) \in [-1, 0, 1]$ that enables it to operate in all four quadrants of v_{Li}, i_L plane which helps in generating $V_{Li} \in \{-V_{B_i}, 0, +V_{B_i}\}$.

In order to simplify the control application, experimentation is carried out by controlling average behavior of switched pack during switching cycle T_{sw}. The duty cycle of each PU thus can be expressed as [25]:

$$u_i(t) := \frac{1}{T_{sw}} \int_{t-T_{sw}}^{t} s_i(\tau) d\tau \tag{4.1}$$

where $u_i(t) \in [-1, 1]$.

4.2 Control Mode

The capability of operation in all four quadrants makes it ideal fit for balancing operations using bi-direction power flow from each PU, however, for this thesis only unipolar mode of switching is considered meaning at a given time either all the PUs are in charging state or discharging state given the direction of $i_L(t)$. For unipolar

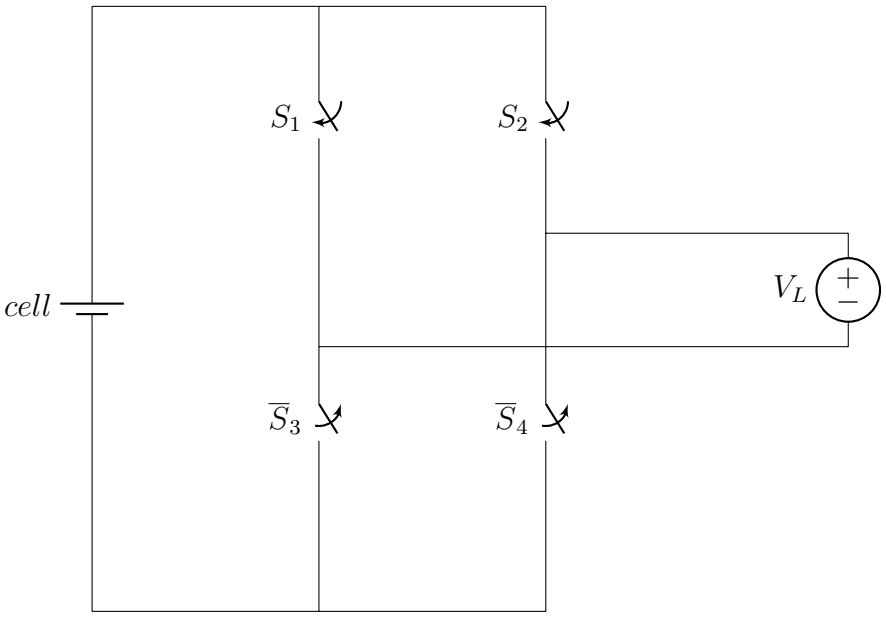

Figure 4.1: Full H-Bridge Module comprising four switches

case duty cycle will be set to $u_i(t) \in [0, 1]$.

4.3 Terminal properties

Average signal on the terminals of each PU is linearly dependent on the duty cycle U_i and is represented with following relation:

$$V_{L_i}(t) = V_{B_i}(t)u_i(t) \tag{4.2a}$$
$$i_{L_i}(t) = i_{B_i}(t)u_i(t) \tag{4.2b}$$

where, V_{L_i} is the terminal voltage and i_{L_i} is the terminal load current of individual PU. V_{B_i} is the terminal voltage of individual battery cell inside PU while i_{B_i} represents current at the input of H-bridge. Similarly terminal power of the whole pack is sum of power from each PU given as $P_L(t) = \sum_{i=1}^{n} P_{L_i}(t)$ with $P_{L_i}(t) = V_{L_i}(t)i_{L_i}(t)$. The average switching behavior is modelled based on the setup used in [25, 29, 30, 53].

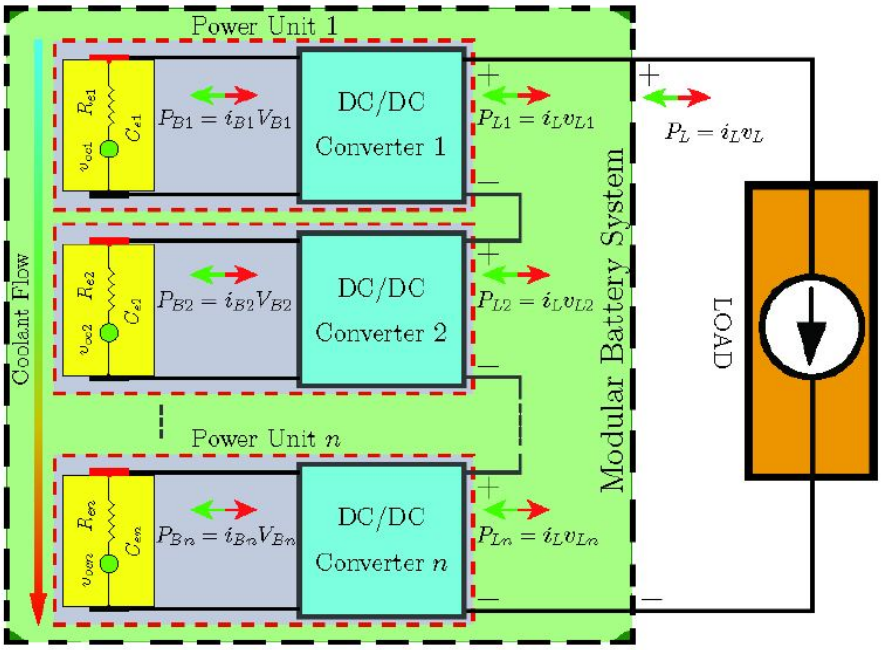

Figure 4.2: Schematic of modular pack consisting of multi-cell/module/pack series configuration

5

System Model

This chapter consists of four subsections. Types of cell models commonly used in literature are presented in 5.1. Electrical and thermal models for the system used in this research work are presented in subsequent sections 5.2 and 5.3 respectively. Last section 5.4 shows the complete system model that integrates both electrical and thermal dynamics.

5.1 Cell Model

5.1.1 Electro-Chemical Model:

The electro-checmical models also know as Particle-Based Distributed are based on thermodynamic and electro-chemical processes of the cell. They give the mathematical representation of the cell using partial differential algebraic equations (PDAEs) which are often highly non-linear and complex. Compared to the other modelling type they offer high accuracy of prediction but they are analytically and computationally inefficient to implement for real-time control problem applications. Some research has been performed to reduce the computational complexity of these models, resulting in distributed-parameter models or lumped-parameter such as expressing the model in the form of differential algebraic equations (DAEs) which can be computationally more efficient as a DAE solver can be used. Although this model is simple and easy to implement however, it rigorous fine-tuning is vital to achieve reliable results. [54]

5.1.2 Grey-Box Model:

Commonly referred to as Equivalent Circuit Model (ECM), this type of modelling technique uses parameterized model and fits input-output experimental data through rigorous fine tuning. The parameterized model can be obtained either through system identification or machine learning techniques such as Artifical Neural Networks, Random Forest Search, Regression etc. to learn parameters of the model that capture relationship between system inputs and outputs. These models are widely used for control applications due to lower computational cost and simplicity despite being less accuracy compared to electro-checmical models and their failure to accurately capture long-term parametric variations due to aging. An odinary differential equation (ODE) based representation makes ECM simple and less computational thus making it a preferred choice for control applications. The ECMs use common electrical elements such as resistors, capacitors along with voltage or current sources

to capture the cell dynamics. Non-linear components can also be used to increase system fidelity. [55, 56].

Since the knowledge of SOC, temperature and battery voltage is captured/ computed through battery dynamics, thus ECM has been selected as the go-to model for this thesis. A first 1-RC ECM has been used in this thesis for control computation [57]. Figure (5.1) shows both Thevenin based 1-RC and 2-RC models.

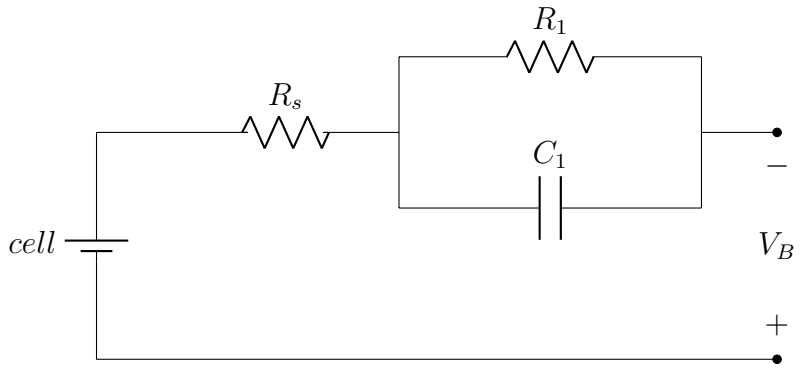

Figure 5.1: 1RC Thevenin Model

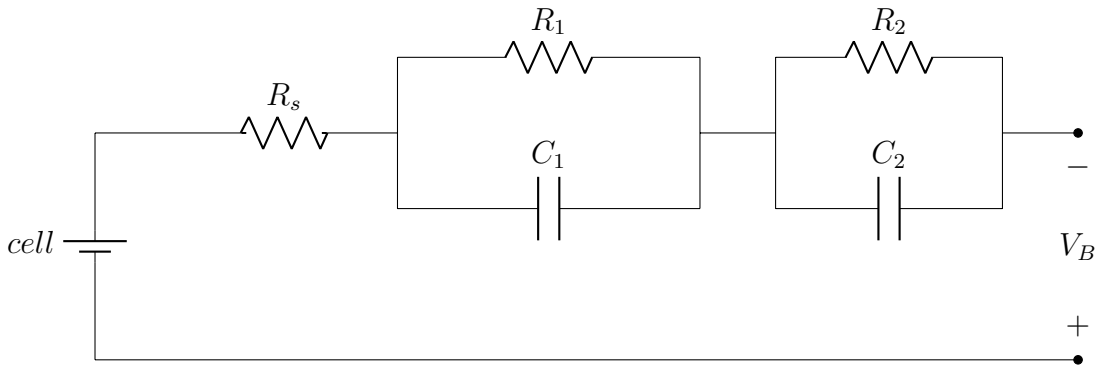

Figure 5.2: 2RC Thevenin Model

The system model of each unit/ cell comprise of three states i.e., SOC (ξ), polarization voltage and temperature. The model has two system outputs namely load voltage V_L and temperature. The dynamics of each state are shown in the proceeding sections.

5.2 Electrical Model

The electrical model deals with the system dynamics pertaining to SOC ξ and polarization voltage V_1 as states while load voltage V_L as output. The electrical model for control application is based on 1-RC Thevenin model shown in figure (5.1) with the assumption that OCV during most of battery operation remains constant [58].

5.2.1 State of Charge

State of charge is represented by following relation:

$$\dot{\xi}_i(t) = m_i I_{Bi}(t), \quad m_i = \frac{\eta_i}{3600 Q_i}, \eta = 1 \tag{5.1}$$

where Q_i is the coulomb capacity of $Cell_i$ while η is the coulomb efficiency. I_{Bi} is the battery cell current given by:

$$I_{Bi}(t) = I_L(t) u_i(t) \tag{5.2}$$

.
Using (5.1) as bases the subsystem for an n-cell battery system can be represented in the following form:

$$\dot{\xi}_i(t) = A_E \xi(t) + B_E I_L(t) u(t) \tag{5.3}$$

where $\xi(t) = [\xi_1(t), \ldots, \xi_n(t)]^T$ is the state vector representing SOC of each cell while $u(t) = [u_1(t), \ldots, u_n(t)]^T$ is control input of each cells output switch.
Matrices A_E and B_E are defined in Appendix A.1.

5.2.2 Polarization Voltage

For the control design the system is considered with 1-RC ECM to represent low frequency dynamics. The polarization resistance R_1 and capacitance C_1 are a function of SOC, temperature and current.
From figure (5.1), using Kirchhoff's current (KCL) and voltage law (KVL), the voltage drop across RC pair can be represented as:

$$\dot{V}_{1,i}(t) = -\frac{V_{1,i}(t)}{R_{1,i} C_{1,i}} + \frac{I_{B,i}(t)}{C_{1,i}} \tag{5.4}$$

The relation in (5.4) can be represented in state-space form as follows:

$$\dot{V}_1(t) = A_{V_1} V_1(t) + B_{V_1} I_L(t) u(t) \tag{5.5}$$

where $V_1(t) = [V_{1,i}, \ldots, V_{1,n}]^T$ is a state vector representing the polarization voltage across each cell.
Matrices A_{V_1} and B_{V_1} are defined in detail in Appendix A.1.

5.2.3 Load Voltage (Output)

Similarly output terminal voltage of each cell i.e., load voltage can also be computed using KCL and KVL as follows:

$$V_{B,i}(t) = V_{OC,i}(t) - V_{1,i}(t) - I_{B,i}(t)R_{s,i}(t) \tag{5.6}$$

The load voltage at respective cell will be:

$$V_{L,i}(t) = V_{B,i}(t)u_i(t) \tag{5.7}$$

The overall system load voltage for cells connected in series in single battery pack can be represented as:

$$V_L(t) = \sum_{i=1}^{n} V_{B,i}(t)u_i(t) \tag{5.8}$$

where $D_V(t) = \sum_{i=1}^{n} V_{B,i}(t) = [V_{B,i}, \ldots, V_{B,n}]$ is a state vector representing the load voltage of each cell.
The relation in (5.6) can be represented in state-space form as follows:

$$V_L(t) = D_V(t)u(t) \tag{5.9}$$

5.3 Thermal Model

Including a battery's thermal model in the system design is necessary for thermal management and better controllability in order to ensure safe working operation within the design limits of the battery. The thermal model deals with changes in heat of the cell during operation and the heat transfer between cell and its surrounding. The heat transfer occurs due to flow of energy from higher Kinectic energy (the cell) to a lower region (the environment) [59]. These temperature changes (heat transfer) occur due to conduction, convection and power losses during operation, briefly defined below:

1. **Conduction:** This phenomenon represents transfer of heat via physical contact. Conduction happens when particles with high (kinectic) energy collide with those with lower energy. These colliding particles then diffuse heat in a disorganized manner until a thermal equilibrium is reached. Conduction deals with heat transfer within the body itself.
2. **Convection:** Convection pertains to heat diffusion from a body to another due to a moving fluid. It not only involves heat diffusion due to conduction but also advection which is transfer by bulk fluid motion. The convection process can either be natural or forced with latter being advection.
3. **Radiation:** Radiation describes transfer of heat from a hotter body to it's surrounding via emission of electromagnetic waves. Principally all matter hotter than absolute zero radiates energy in its surrounding at a rate proportional to temperature difference.

For in-depth knowledge an enthusiastic reader can refer to [59, 60].
An accurate thermal model for control and thermal balancing purposes also takes into account the influence of cooling methods and techniques as well [61]. The thermal model for this thesis is based on lumped model presented in [62], however in this case all the temperature nodes are kept independent for each other meaning coolant only passes through only one cell in its path.

The thermal model considered during this thesis is based on following assumptions:

- It is a lumped capacitance model for prismatic LiB cells using flow network modelling approach technique [63, 59].
- The coolant exhibits laminar flow with constant known inlet temperature.
- Coulombs losses are ignored in this work as Columbic efficiency is considered $\eta = 1$. However, this can easily be incorporated into the system without any major changes required.
- The cell parameters are usually non-linear function of temperature however, for simplification purposes they are assumed constant for control design [64]. This is a fairly reasonable assumption due to very little variation in cell resistance under normal operating range [25^{o}C, 40^{o}C].

Given these assumptions, mathematical representation is as follows:

$$C_{t,i}\dot{T}_i(t) = Q_i + \frac{T_f - T_i(t)}{R_{t,i}} + \frac{T_{amb} - T_i(t)}{R_{u,i}} \tag{5.10}$$

where T_f is the constant known coolant inlet temperature, $C_{t,i}$ is the lumped heat capacity, $R_{t,i}$ is the convection (thermal) resistance of the cell while $R_{u,i}$ is the convection (thermal) resistance of cell casing. The convection can be modelled in different ways [65, 66] and is dependent on coolant type and flow rate. Q_i is the heat generation in a battery cell that can be approximated as sum of irreversible and reversible heat generation [63][67].

$$Q_i = Q_{irreversible} + Q_{reversible} \tag{5.11}$$

- **Irreversible heat generation:** This type of heating is based on power losses within a battery cell when the current flows through it due to impedance. This can simply be modelled with the help of following equation:

$$\begin{aligned} Q_{irreversible} &= (V_{B,i} - V_{OC,i})I_{B,i}(t) && (5.12)\\ &= (V_{OC,i} - V_{1,i} - I_{B,i}(t)R_{s,i} - V_{OC,i})I_{B,i}(t) && (5.13)\\ &= (-V_{1,i} - I_{B,i}(t)R_{s,i})I_{B,i}(t) && (5.14)\\ &= -V_{1,i}I_{B,i}(t) - I^2_{B,i}(t)R_{s,i} && (5.15) \end{aligned}$$

  The first term is (5.15) is the power losses across parallel RC in 1-RC model while second term refers to ohmic losses due to cell's internal resistance. The term $I^2_{B,i}$ can be approximated by rms current under switching $I^2_L u_i(t)$ flowing through the respective cell.

- **Reversible heat generation:** Entropic losses occurring due to endothermic and exothermic chemical reactions and represent the loss of energy in the form of heat, often under a reversible process, influencing temperature of the system. In simple terms this losses arise due to movement of lithium ions in and out of the electrodes. Ideally these heat changes are minuscule thus it is a common practice to ignore these losses for xEV applications [68, 69, 63, 70], however, in this work as a more practical approach entropic losses are incorporated into the model using the experimental data obtained by measuring reversible voltage curve (in relation to OCV) for different SOC values [71]. Reversible heat losses can account anywhere from 5% - 20% heat losses during the operation[72]. Thus, the reversible heat generated in a cell can be computed using following expressions [67, 73]:

$$Q_{reversible} = \frac{\partial V_{OC}}{\partial T} T_i(t) I_{B,i}(t) = q_{rev,i} T_i(t) I_{B,i}(t) \tag{5.16}$$

$$Q_{reversible} = Q_r I_{B,i}(t) \tag{5.17}$$

  where V_{OC} is a function of SOC and temperature.

For practical purposes Q_r is taken from the look-up table provided as data. From the above relations in eq. (5.10), (5.17) and (5.15) one can find:

$$\dot{T}_i(t) = \frac{-V_{1,i}(t) I_{B,i}(t) - I_{B,i}(t)^2 R_{s,i}(t) + Q_r I_{B,i}(t)}{C_{t,i}} + \frac{T_f - T_i(t)}{R_{ti} C_{ti}} + \frac{T_{amb} - T_i(t)}{R_{u,i} C_{ti}} \tag{5.18}$$

$$= \left[-\frac{1}{R_{ti} C_{ti}} - \frac{1}{R_{u,i} C_{ti}} \right] T_i(t) + \frac{-V_{1,i}(t) I_{B,i}(t) - I_{B,i}(t)^2 R_{s,i}(t) + Q_r I_{B,i}(t)}{C_{t,i}} + \frac{1}{R_{u,i} C_{ti}} T_{amb} + \frac{1}{R_{t,i} C_{ti}} T_f \tag{5.19}$$

The relation in (5.19) can be represented in state-space form as follows:

$$\dot{T}(t) = A_T(t) T(t) + B_T(t) I_L(t) u(t) + E_T(t) \begin{bmatrix} T_f \\ T_{amb} \end{bmatrix} \tag{5.20}$$

$$= A_T(t) T(t) + B_T(t) I_L(t) u(t) + E_T(t) w \tag{5.21}$$

where $w = \begin{bmatrix} T_f \\ T_{amb} \end{bmatrix}$. Matrices A_T, B_T, and E_T are defined in Appendix A.1.

The temperature state is also observed as the output of the system along with load voltage.

5.4 Complete System Model

The complete continuous-time electrothermal state-space model representation of the system with n-cell series module battery unit is expressed using following state-

space system:

$$\dot{x}(t) = Ax(t) + BI_L(t)u(t) + Ew \tag{5.22a}$$
$$y(t) = Cx(t) + Du(t) \tag{5.22b}$$

where $x(t) = [\xi^T(t), V_1(t)^T, T(t)^T]^T \in \mathbb{R}^{3n}$ is the state vector while $y(t) = [T(t)^T, V_L(t)^T]^T \in \mathbb{R}^{2n}$ is the output vector. Refer to Appendix A.1 for definition of all the system matrices in (5.22)
.

5.4.1 Model Discretization

For control purpose continuous-time model in ((5.22)) has to be transformed to discrete form using Euler approximation for a fixed sampling interval $[kh, (k+1)h]$, with h being the step size and assumption $I_L(k)$ being constant during the sampling interval [74]. The discrete-time model is represented as:

$$x(k+1) = x(k) + h * [A_d x(k) + B_d u(k) + E_d w] \tag{5.23a}$$
$$y(k) = Cx(k) + Du(k) \tag{5.23b}$$

6
Control Scheme

In this chapter control scheme has been presented. In the first part section 6.1 a definition of objective function for less familiar readers is presented. In the second part section 6.2 objective function used in this thesis is formulated in a convex fashion. Section 6.3 defines the global optimal control problem used in this thesis. In section 6.4 different control strategies to be explored in this work are presented.

6.1 Objective Function

The primary objective of this thesis to maximize power availability to the system and ensure optimal utilization of power availability of each individual cell and/or battery pack for optimal performance and long life. The maximization of SoP has been incorporated through minimization of SoC and thermal imbalance in the objective function for this thesis work.
The control scheme comprises of two parts:

- Objective Function
- Constraints

6.1.1 Objective Function

Objective function, comprising a function of states and control variables, finds the optimal control law for a given optimization problem. The objective function also known as cost function is a scalar value that tries to find a solution based on current states that will give a minimum scalar value as output.

6.1.2 Constraints

Constraints are used to define limitations of the system, outline a safe operating range and check system feasibility in real environment.

6.2 Convex Problem Formulation

The control objective for this work includes SoC balancing and thermal balancing across the pack using minimum control effort that fulfills power demand and increases systems power capability through minimzation of SoC and thermal imbalance. Full drive cycle information is considered known for the problem formulation and all the values are accessible. The control problem is constructed as a standard

Linear-Quadratic Problem (LQP) for the system proposed in section 5. The objective function is well motivated with polyhedra constraint formulation to transform the optimization problem as standard LQ one. The formulation in this section is based on [25].

6.2.1 Non-Standard Form

The objective function is geared towards SOC and thermal balancing along with minimizing the control effort to find the optimal solution that indirectly maximizes power capability of the system.

In order to achieve the SOC and thermal balancing the objective function attempts to minimize error among relevant states of all cells within an individual battery pack. Thus in order for the objective function to find minimum value the absolute error between respective states must be (ideally) zero.

The problem formulation can thus be achieved by deriving error vectors for SOC and thermal states that can be incorporated into the objective function.

6.2.1.1 Error Vectors

Lets take the example of SOC error vector where we have state vector comprising SOC of each individual cell within a single pack i.e., $\xi(t) = [\xi_1(t), \ldots, \xi_n(t)]^T$. The error vector can be defined as follows then [25]:

$$e_\xi(k) = \xi(k) - \overline{\xi}(k) \cdot 1_n = M_e \xi(k) \tag{6.1}$$

$$M_e = (I_n - \frac{1}{n} 1_{n \times n}) \in R^{n \times n} \tag{6.2}$$

where $\overline{\xi}(k)$ is the mean of SOC state vector $\xi(k)$ and matrix M_e is used to map the state vector to its corresponding error vector. The error vector for temperature state can also be formulated in similar way, which will give us the following expression [25]:

$$e_T(k) = T(k) - \overline{T}(k) \cdot 1_n = M_e T(k) \tag{6.3}$$

6.2.1.2 Objective Function Terms

The objective function is further categorized into different terms each focusing on different aspect/target of the defined objective. Overall objective function is simply the sum of all these sub-objectives define below.

6.2.1.2.1 SOC balancing: The SOC balancing term is designed to minimize the error between SOC of each individual cell and is expressed as follows [25]:

$$J_E = \sum_{k=0}^{N-1} \|e_\xi(k)\|^2_{Q_E} + \|e_\xi(N)\|^2_{P_E} \tag{6.4}$$

6.2.1.2.2 Thermal balancing: Thermal balancing term is designed to minimize the error between temperature of each individual cell and is expressed as follows [25]:

$$J_T = \sum_{k=0}^{N-1} \|e_T(k)\|^2_{Q_T} + \|e_T(N)\|^2_{P_T} \tag{6.5}$$

6.2.1.2.3 Peak temperature: As can be seen via eq (6.5) that objective function aims at reducing the temperature difference among all cells but this can lead a scenario where in order to achieve thermal balancing the objective function might come up with a solution that leads to overall high temperature of the battery pack which can deteriorate the systems performance and power capability. Battery packs operating at high temperature can age considerably faster and are also at risk of thermal runway [75]. It is also observed that high temperature results in increased degradation and earlier end of life (EoL) of a cell[76]. Thus, in order to reduce overall temperature of the system additional term is introduced below in eq. (6.6) for this purpose [25]:

$$J_{\overline{T}} = \sum_{k=0}^{N-1} \left\|\overline{T}(k)\right\|^2_{Q_{\overline{T}}} + \left\|\overline{T}(N)\right\|^2_{P_{\overline{T}}} \tag{6.6}$$

6.2.1.2.4 Control Input: One of the tasks achieved via the objective function is that of minimizing the overall control effort while fulfilling all of the set targets [25]:

$$J_u = \sum_{k=0}^{N-1} \|u(k)\|^2_{R_u} \tag{6.7}$$

6.2.1.2.5 Control Move Restriction: In this work effects of imposing control move restriction will be explored against system performance in delivering demanded power. A hard constraint in this regard might lead to in-feasibility thus a slack variable will be introduced and fine tuned to see how the system performs.

$$J_{\Delta u} = \sum_{k=0}^{N-1} \Delta u(k) \tag{6.8}$$

6.2.1.2.6 Power demand slack: Effects of hard control move restrictions will also be studied by relaxing constraints on power demand so that optimization problem in-feasibility can be avoided if system is unable to meet all the set constraint requirements.δV_L is the slack used to relax constraints on voltage demand.

$$J_{\delta V_L} = \sum_{k=0}^{N-1} \delta V_L(k) \tag{6.9}$$

From equations (6.4)-(6.9) the overall objective function can be constructed as follows:

$$J = \gamma_1 J_E + \gamma_2 J_T + \gamma_3 J_{\overline{T}} + \gamma_4 J_u + \gamma_5 J_{\Delta u} + \gamma_6 J_{\delta V_L} \tag{6.10}$$

The γ_i are weights introduced to signify importance of one objective over the other and can be fine tuned based on the expected outcome. The different control models explored in this work are discussed in a later subsection 6.4.3.

6.2.2 Standard Form

The objective function can be expressed in standard state space form described in (5.23) as follows:

$$J = \sum_{k=0}^{N-1} [\|x(k)\|^2_{\overline{Q}_x} + \|u(k)\|^2_{\overline{R}_u}] + \|x(N)\|^2_{\overline{P}_x} + \sum_{k=0}^{N-1} \Delta u(k) + \sum_{k=0}^{N-1} \delta V_L(k) \tag{6.11}$$

6.2.2.1 Penalty Matrices

In eq. (6.11) $\overline{Q}_x$, $\overline{P}_x$ and $\overline{R}_u$ are the penalty matrices that are symmetric positive (semi-)definite. The matrix $\overline{Q}_x$ is the running state penalty matrix, $\overline{P}_x$ being the terminal state penalty matrix and $\overline{R}_u$ referring to control input penalty. In a LQR problem these penalty matrices are used to define weights of states and inputs in the objective function itself.

6.2.2.1.1 State Penalty Matrices: The penalty matrices definition used in eq. (6.11) are shown below in eq. (6.12)

$$\overline{Q}_x = \text{blkdiag}(\gamma_1\overline{Q}_E, 0, \gamma_2\overline{Q}_T, \gamma_3\overline{Q}_{\overline{T}}) \tag{6.12a}$$
$$\overline{P}_x = \text{blkdiag}(\gamma_1\overline{P}_E, 0, \gamma_2\overline{P}_T, \gamma_3\overline{P}_{\overline{T}}) \tag{6.12b}$$
$$\overline{Q}_E = M_e^T Q_E M_e \tag{6.12c}$$
$$\overline{Q}_T = M_e^T Q_T M_e \tag{6.12d}$$
$$\overline{Q}_{\overline{T}} = M_e^T Q_{\overline{T}} M_e \tag{6.12e}$$
$$\overline{P}_E = M_e^T P_E M_e \tag{6.12f}$$
$$\overline{P}_T = M_e^T P_T M_e \tag{6.12g}$$
$$\overline{P}_{\overline{T}} = M_e^T P_{\overline{T}} M_e \tag{6.12h}$$

6.2.2.1.2 Control Input Penalty Matrix: The matrix $\overline{R}_u$ defines weights on control input. It has been shown that the balancing algorithm mostly manipulates this penalty matrix [77] to achieve objective. The mere definition of this matrix gives rise to several control strategies that are discussed in the relevant subsection 6.4.

6.3 Global Optimal Control Problem

The global optimal control problem for the complete function can thus be expressed as depicted in following subsection.

6.3.1 Controller for Ideal Load Management

The objective function along with applicable constraints is as follows [25]:

$$\begin{aligned}
&\textit{minimize} \quad J(x(0), u(0:N_d-1)) && (6.13a)\\
&\quad \textit{subject to}\\
&\quad x(k+1) = A_d x(k) + B_d u(k) + E_d w(k) && (6.13b)\\
&\quad D_v(k)u(k) = V_{Ld}(k) = \alpha n_c V_{min} && (6.13c)\\
&\quad \xi(k) \in \chi_{E_g}, \forall k && (6.13d)\\
&\quad T(k) \in \chi_{T_g}, \forall k && (6.13e)\\
&\quad u(k) \in \mathcal{U} = \{u(k) | H_u u \leq h_u\} \qquad H_u = vertcat(I_n, -I_n) && (6.13f)\\
&\quad \Delta u \leq u_{max} && (6.13g)\\
&\quad k \in \mathcal{K} = \{0, \ldots, N_d - 1\} && (6.13h)
\end{aligned}$$

6.4 Control Strategy:

Different control strategies are proposed here with one pertaining to conventional battery system while the rest corresponding to optimal control methodology of reconfigurable battery systems. All these schemes are discussed below[78]:

6.4.1 Uniform Duty Cycle

In uniform duty cycle (UDC) scheme the load requirement is distributed to all cells equally regardless of their power capabilities. Advantages of this scheme are simpler control however this control strategy fails to meet the objective of maximizing power capabilities of the system if the heterogeneities are pronounced. In this control strategy the control input penalty matrix is set to identity. In this thesis, UDC is used to gather results for conventional battery system controls scheme. It will serve as a benchmark for comparison with RBS control scheme.

6.4.2 Balancing with Active Control

In this strategy the balancing is achieved by distributing load requirements on each cell as per its current power capability based on SoC of each cell. The advantage of this scheme is its ability to maximize power delivery over the drive cycle as opposed to UDC however this also means control model is complex. This scheme corresponds to control of RBS. The selection of R matrix can be made in three following ways for this case:

6.4.2.1 Balancing during charge phase

In this strategy balancing is only pursued during the charging phase thus R matrix is set in such a manner that during charging phase control cost on cells with high charge capacity (SoC) will be lower while higher on cells with lower charge capacity. The disadvantage here is that this strategy is only useful for drive cycles with regular and significant charging phases as compared to discharge phase. The R matrix during charging phase will be diagonalized matrix of SoC of each cell rescaled to range [0, 1]. The R matrices for charging and discharging phase will look like:

$$R_{charge} = \begin{bmatrix} \xi_1 & 0 & 0 \\ 0 & \xi_2 & 0 \\ 0 & 0 & \xi_3 \end{bmatrix} \in [0, 1] \tag{6.14}$$

$$R_{discharge} = \begin{bmatrix} 1 & 0 & 0 \\ 0 & 1 & 0 \\ 0 & 0 & 1 \end{bmatrix} \tag{6.15}$$

6.4.2.2 Balancing during high charge phase

The balancing action is only incorporated here during phases of high charging in order to reduce frequency of switching. The R matrix is set in the similar manner as section 6.4.2.1. The advantage is reduced switching frequency and harmonics associated with it but just like the previous strategy here too it is only useful for drive cycles with regular and significant high charging phases as compared to discharge phase.

6.4.2.3 Balancing during entire drive cycle

In this control strategy balancing action is applied during the entire drive cycle with different R matrix for charging phase $+I$ and separate one for discharging phase $-I$. In this method, during discharging phase cells with high discharge capacity will have lower control cost while for charging phase cells with higher charge capacity will have lower control cost. The control matrix R is similarly rescaled to range [0, 1]. The advantage is significantly faster balancing compared to previously described strategies however at the cost of switching between two different control schemes throughout the drive cycle. This control schema is used for experimentation during this thesis work.

$$R_{charge} = \begin{bmatrix} \xi_1 & 0 & 0 \\ 0 & \xi_2 & 0 \\ 0 & 0 & \xi_3 \end{bmatrix} \in [0, 1] \tag{6.16}$$

$$R_{discharge} = \begin{bmatrix} \frac{1}{\xi_1} & 0 & 0 \\ 0 & \frac{1}{\xi_2} & 0 \\ 0 & 0 & \frac{1}{\xi_3} \end{bmatrix} \in [0, 1] \tag{6.17}$$

6.4.2.4 Customized balancing

This strategy is advanced form of the scheme described in section 6.4.2.3 using multiple R matrices to achieve faster balancing for different charge and discharging rates.

6.4.3 Control Model

6.4.3.1 Model 1

This model uses the objective function as eq. (6.18) this can be used to create control model for all the control schemes with hard constraints on power demand and none on the control move restriction [25].

$$J = \gamma_1 J_E + \gamma_2 J_T + \gamma_3 J_{\overline{T}} + \gamma_4 J_u \tag{6.18}$$

6.4.3.2 Model 2

Model shown in eq. (6.19) can be used to relax the hard constraint on control move restriction and see its effects on optimization problem feasibility [25].

$$J = \gamma_1 J_E + \gamma_2 J_T + \gamma_3 J_{\overline{T}} + \gamma_4 J_u + \gamma_5 J_{\Delta u} \tag{6.19}$$

6.4.3.3 Model 3

This model employees hard constraint on control move while softens the constraints on voltage demand and is shown in eq. (6.20) [25].

$$J = \gamma_1 J_E + \gamma_2 J_T + \gamma_3 J_{\overline{T}} + \gamma_4 J_u + \gamma_5 J_{\delta V_L} \tag{6.20}$$

7

Results

The simulations setup and associated results are discussed in detail in this section. Simulation model referred to as **control-oriented model** is developed in Matlab and Simulink environment. YALMIP [79] toolbox is used to solve the optimization problem in Matlab. All the parameters used are extracted from look-up tables provided by Volvo Group based on lab experimental data. Based on the data provided:

- V_{OC} is function of SOC and temperature
- R_s, R_1, R_2, C_1, and, C_2 are function of SOC, temperature and current.
- $Q_{reversible}$ ($\frac{\partial V_{OC}}{\partial T}$) is a function of V_{OC} and SOC.

Constraints shown in table (7.1) were imposed for bounding the optimization problem and defining feasible region. Load profile provided by Volvo and used for experimentation is shown in figure (7.1).

Parameter	**Notation**	**Symbol**	**Lower Bound**	**Upper Bound**
SOC	ξ	nu	0	1
Temperature	T	^oC	0	40
Terminal Voltage	V	V_B	3.0	4.2
Terminal Current	A	I_B	-150	+150
Input actuator	u	nu	0	1
Slew rate	Δu	nu	-	0.1

Table 7.1: System constraints for the optimization problem

The model starts with an initial state, optimization problem is solved based on the current state information and control input is computed. States are updated according to this control input and sequence continues for future time steps.

Both the models contain three cells connected in series with each other in a pack with individual switches isolating them from load.

All the results presented here are based on one step predictor horizon since it was found that increasing the length of prediction horizon results in increasing the computational time. It was also observed that one step predictor produced considerably good results when compared with higher horizon thus justifying the use.

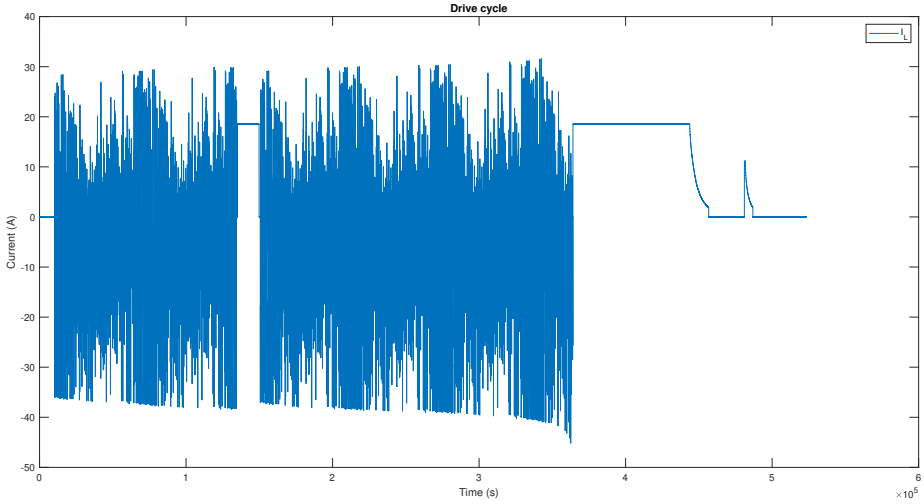

Figure 7.1: Load profile used for experimentation

Parameter	Value
SoC	[0.95, 0.85, 0.75]
Temperature	[23, 25, 27] ^oC
SoR	[1, 1, 1]
SoH	[1, 1, 1]
V_{Ld}	8.1 V

Table 7.2: UDC experimental setup

7.1 Conventional Battery System - Single Pack (UDC)

This setup has a single battery pack comprising three battery cells connected in series. Since all the cells follow UDC, this means freedom to control each cell individually as per its power capability doesn't exist and the probability of any cell violating constraints is much higher. The experimental parameters are as per table 7.2.

As it can be seen from figure (7.9) that all the cells have the exact same duty cycle resulting in all the cells regardless of there current state will contribute the equal ratio towards the power demand. This leads to imbalance of SoC remaining constant as can be seen in the evolution of SoC from figure (7.2) and error in SoC of each cell with overall pack average in figure (7.4). It is pertinent to note here that the solution becomes infeasible towards the end since cell 1 reaches the maximum threshold set for SoC. An interesting observation can be seen in the thermal behavior of the system which leads to all the cells despite having different initial temperature eventually converge to same level depicted in temperature curve figure (7.3) and error with average pack temperature figure (7.5). This is mainly due to the way the thermal model has been constructed. Since in the thermal model the inlet

coolant temperature is assumed to be constant 25^oC and thermal transfer among cells is neglected thus the thermal balancing is inevitable here. This points to a potential future work research area of incorporating thermal coupling between cells as performed in [25]. However, during through the drive cycle the setup does fulfill the power demand as shown in figure (7.6) and error between terminal voltage and demand in figure (7.8).

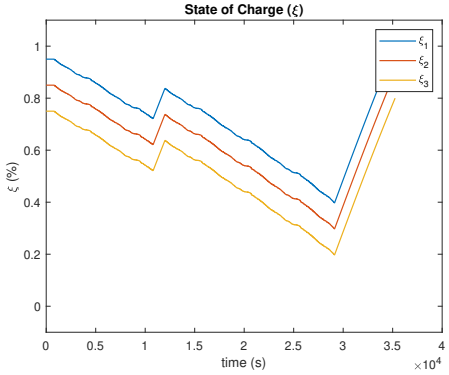

Figure 7.2: SOC for UDC

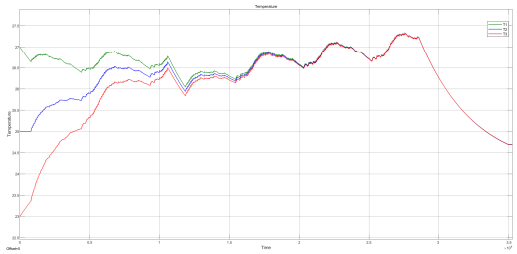

Figure 7.3: Temperature for UDC

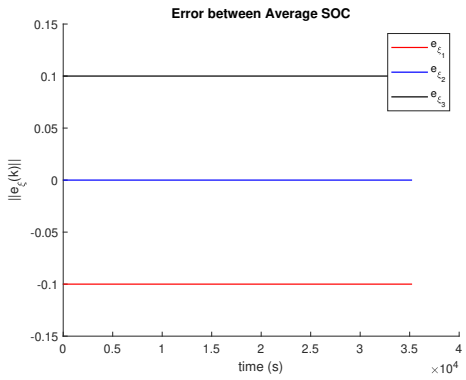

Figure 7.4: Error in SOC among cells for UDC

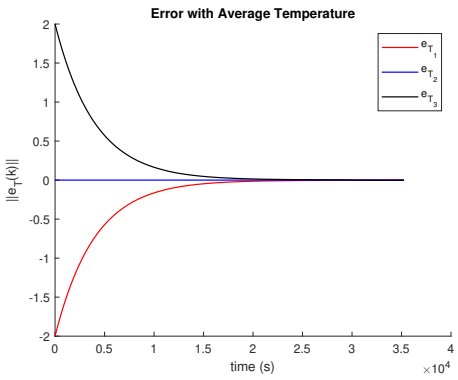

Figure 7.5: Error in Temperature among cells for UDC

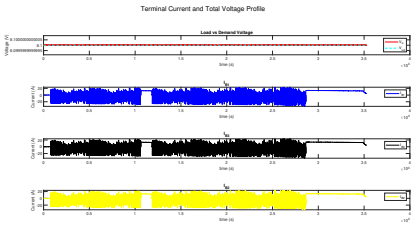

Figure 7.6: Total load voltage and current through individual cells for UDC

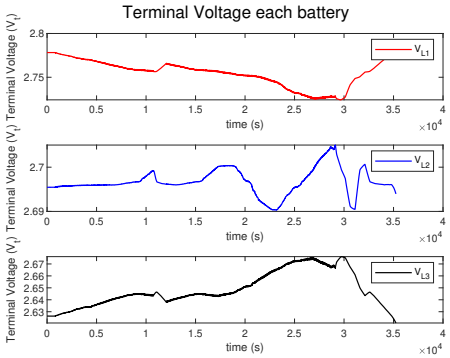

Figure 7.7: Terminal voltage of each cell in the pack for UDC

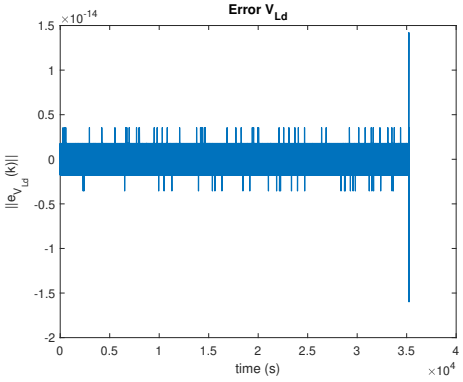

Figure 7.8: Error between terminal voltage of pack vs demand for UDC

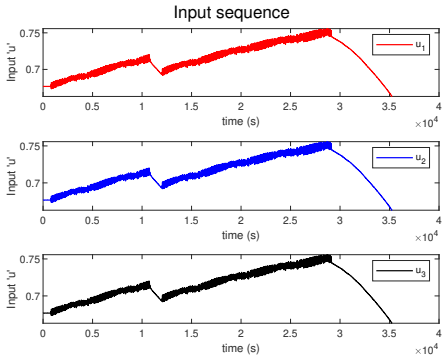

Figure 7.9: Input sequence for each cell for UDC

7.2 Balancing with Active Control - Single Pack

As mentioned earlier, the control scheme described in 6.4.2.3 is used to study the effectiveness of reconfigurable control of battery system. As mentioned earlier the balancing is achieved here during the entire drive cycle with a separate input penalty matrix for charging and discharging phases of the cycle in such a manner to maximize the power capability of whole system and obtain faster balancing across the system. The criterion for balancing is set as follows [80]:

- **SOC Balancing:** SOC difference within 2% between max and min values across complete unit.
- **Temperature Balancing:** Temperature difference within $\pm 1^oC$ between max and min values across complete unit.

7.2.1 Control Models

As explained in section 6.4.3 different control models are tested in this thesis work. Results of all these models are presented and analyzed in following subsections.

Parameter	Value
SoC	[0.95, 0.85, 0.75]
Temperature	[23, 25, 27] ^oC
SoR	[1, 1, 1]
SoH	[1, 1, 1]
V_{Ld}	8.1 V

Table 7.3: Scenario 1 experimental setup

7.2.1.1 Model 1

In this control model, there is hard constraint on power output that must be fulfilled however there exists no restriction on control input of each individual unit. This means all the cells are capable of operate between $u = [0, 1]$. The objective function for this control model is expressed in eq. (6.18).

7.2.1.1.1 Scenario 1 In this setup the heterogeneity exist in the initial states SoC and Temperature while the SoR and SoH are same for all cells as shown in table 7.3. Here two different cost penalty matrices R for input are used, one for charge and the other for discharge phase. These matrices are kept generic without any fine-tuning and are shown in eq. (7.1). This ensures that during the discharge cycle the cell with higher SoC will contribute more while during the charge phase the cell with lower SoC will contribute more to achieve energy balancing.

$$R_{\text{ch}} = \text{rescale}(\text{inv}(\text{diag}(\text{SoC}(1{:}\text{nc})))) \tag{7.1a}$$
$$R_{\text{dch}} = \text{rescale}(\text{diag}(\text{SoC}(1{:}\text{nc}))) \tag{7.1b}$$

It can be seen in SoC curve figure (7.10) and error among cells SoC in figure (7.12) that system does fairly good job at converging the energy of all cells to set limits of 2% SoC difference limit and maintains it through out the drive cycle once this balancing has been achieved at around 10,000 seconds mark. Thermal behaviour figure 7.11 and figure 7.13 remains same due to the reasons explained earlier in section 7.1. Since the load profile shown in figure (7.1) comprises of fluctuations between *+ve* and *-ve* currents thus from figures (7.17) and (7.15) the contribution difference between cell 1 (strongest pack cell) and cell 3 (weakest pack cell) are similar something that will be more pronounced when control move restrictions will be imposed later in sections 7.2.1.2 and 7.2.1.3. The setup fulfills the demand voltage throughout the drive cycle successfully as shown in figures (7.14) and (7.16).

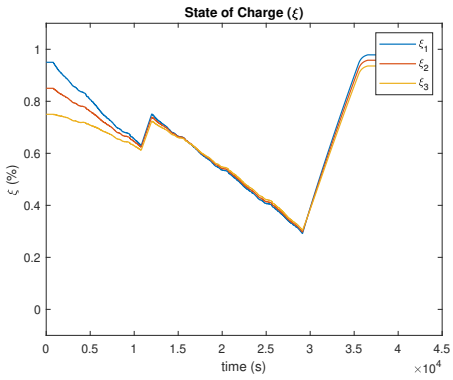

Figure 7.10: SOC for Model 1 - Scenario 1

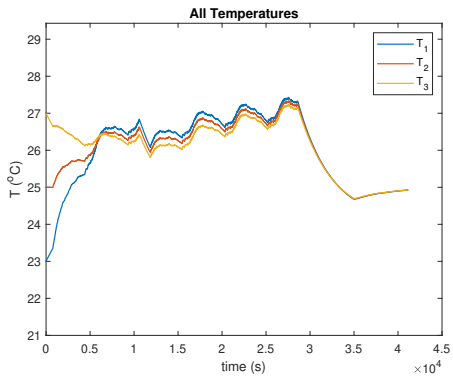

Figure 7.11: Temperature for Model 1 - Scenario 1

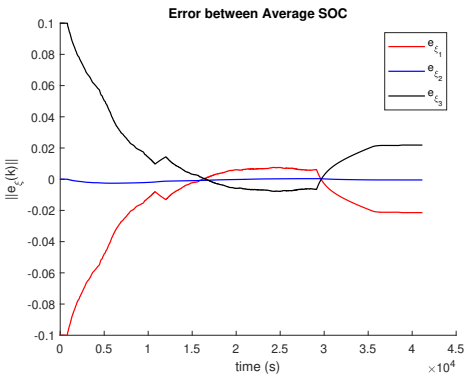

Figure 7.12: Error in SOC among cells for Model 1 - Scenario 1

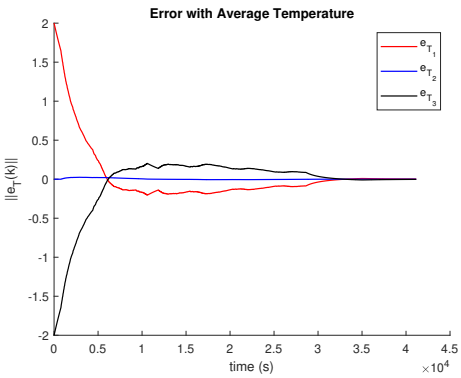

Figure 7.13: Error in Temperature among cells for Model 1 - Scenario 1

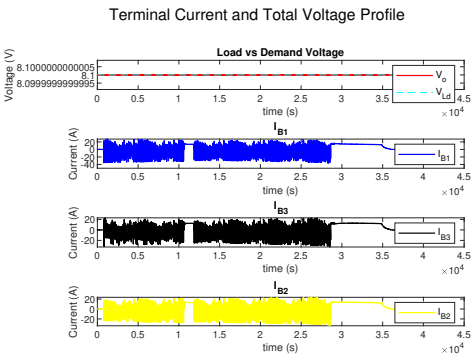

Figure 7.14: Total load voltage and cell current for Model 1 - Scenario 1

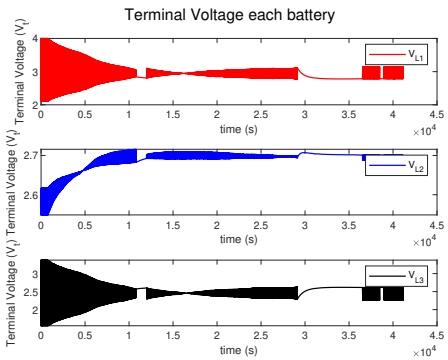

Figure 7.15: Terminal cell voltage for Model 1 - Scenario 1

Parameter	Value
SoC	[0.75, 0.75, 0.75]
Temperature	[25, 25, 25] ^oC
SoR	[1, 1.2, 1.4]
SoH	[1, 0.9, 0.8]
V_{Ld}	8.1 V

Table 7.4: Scenario 2 experimental setup

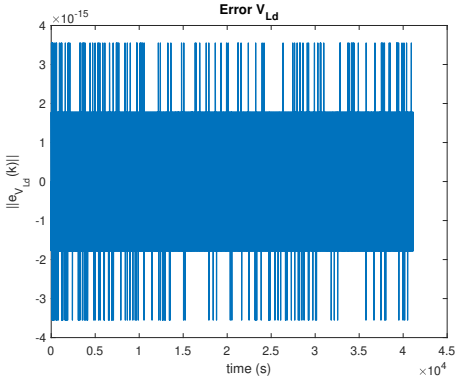

Figure 7.16: Error terminal voltage vs demand for Model 1 - Scenario 1

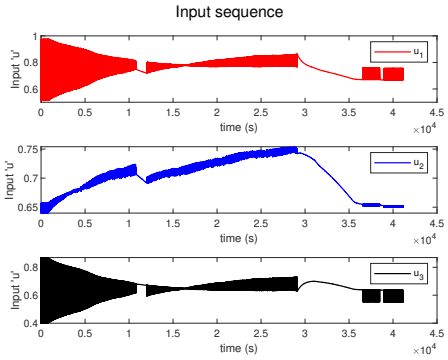

Figure 7.17: Input sequence for each cell for Model 1 - Scenario 1

7.2.1.1.2 Scenario 2 In this setup the initial states SoC and Temperature are same for each cell of the pack while the SoR and SoH vary to create heterogeneity as shown in table 7.4:

Same penalty matrices R are used for this scenario as well as in scenario 1 (section 7.2.1.1.1) and eq. (7.1). It can be seen that the performance of the system in terms of energy balancing is not as satisfactory as the requirements imposed for SoC difference among cells to be within ±2%. In SoC evolution figure (7.18) and SoC error figure (7.20) the energy imbalance in system increases continuously during the dominant discharge phase while it reduces rapidly during dominant charging phase. This is due to the heterogeneities in cells having different SoR and SoH values. It becomes difficult for the system to maintain balance in the energy with generic input penalty matrix that worked well for Scenario 1 in section 7.2.1.1.1. Thermal behavior although does converge due to system model as explained in section 7.1 however the behavior is different to that seen in results from section 7.2.1.1.1. The thermal profile for this experiment shown in figures (7.19) and (7.21) varies from the scenario 1 profile shown in figures (7.11) and (7.13) due to all the cells not being uniform and difference in SoR now effects the thermal properties of the cell due to change in resistance. Nonetheless system meets the voltage demand effectively as illustrated in figures (7.22) and (7.24). Individual cell contribution shown in figures (7.25) and (7.23) is hard to distinguish due to load profile used as explained earlier in section 7.2.1.1.2.

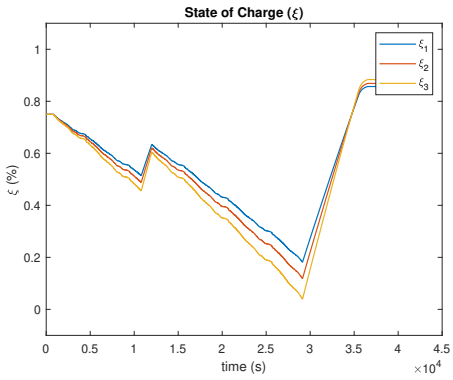

Figure 7.18: SOC for Model 1 - Scenario 2

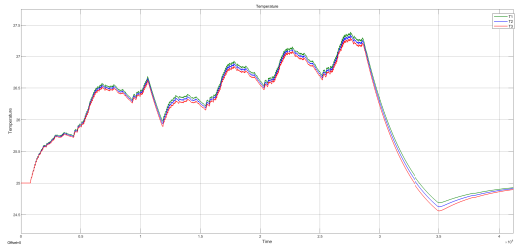

Figure 7.19: Temperature for Model 1 - Scenario 2

Figure 7.20: Error in SOC among cells for Model 1 - Scenario 2

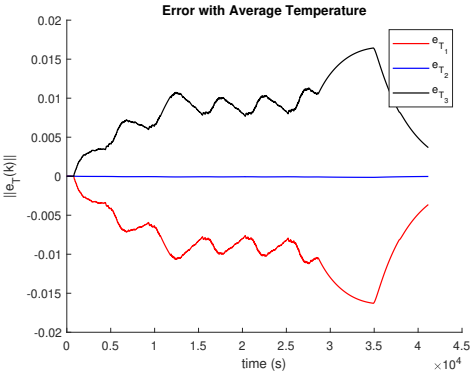

Figure 7.21: Error in Temperature among cells for Model 1 - Scenario 2

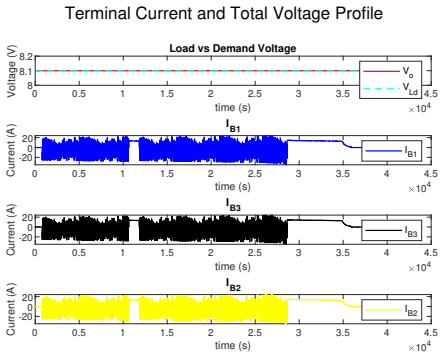

Figure 7.22: Total load voltage and cell current for Model 1 - Scenario 2

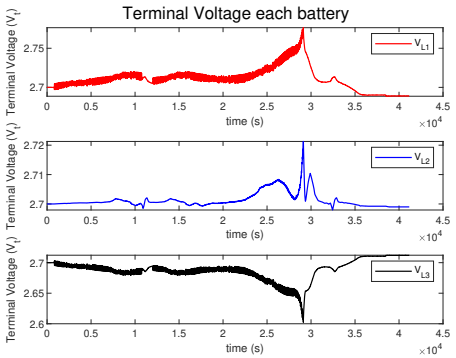

Figure 7.23: Terminal cell voltage for Model 1 - Scenario 2

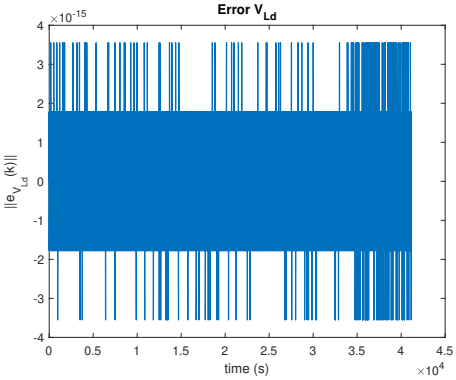

Figure 7.24: Error terminal voltage vs demand for Model 1 - Scenario 2

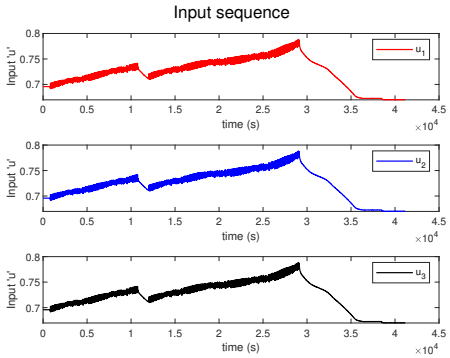

Figure 7.25: Input sequence for each cell for Model 1 - Scenario 2

7.2.1.1.3 Scenario 3 This setup is similar to Scenario 2 with difference of tuning to achieve better balancing results. All the parameters for this experiment are same as scenario 2 shown in table 7.4. It can be seen here that system performance has improved significantly and works well despite the heterogeneties considered. Good tuning of input penalty matrix ensures excellent balancing throughout the drive cycle despite significant differences in all cells parameters. An SoC difference of $\pm 10^{-3}$ is maintained successfully throughout the drive cycle as illustrated in figures (7.26) and (7.28). The system manages to fulfill the power demand successfully as shown in figures (7.30) and (7.32). Since the input penalty matrix is fine tuned for the give cell conditions, the difference in contributions is more prominent here as seen in figures (7.33) and (7.31). It can be observed that cell 1 being the stronger cell in terms of charge capacity contributes more during the drive cycle while the weakest cell 3 contributing the least. As most of the load is borne by strongest cell this means effects of parametric difference among cells will not further accelerate since weaker cells are contributing less here.

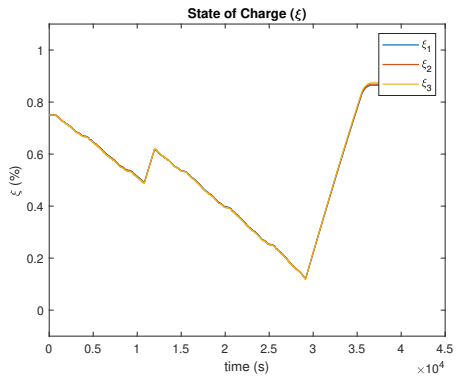

Figure 7.26: SOC for Model 1 - Scenario 3

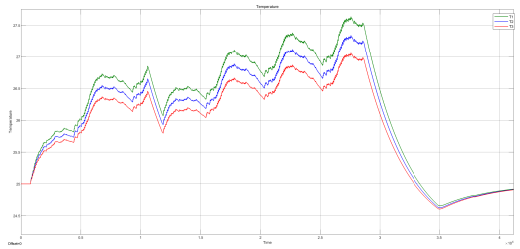

Figure 7.27: Temperature for Model 1 - Scenario 3

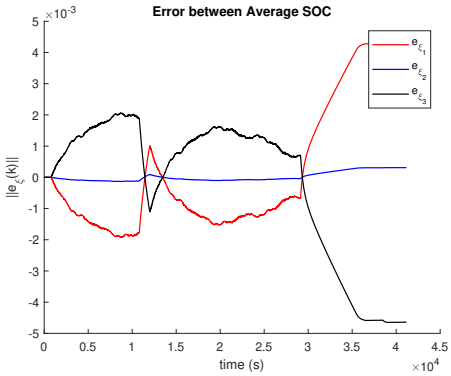

Figure 7.28: Error in SOC among cells for Model 1 - Scenario 3

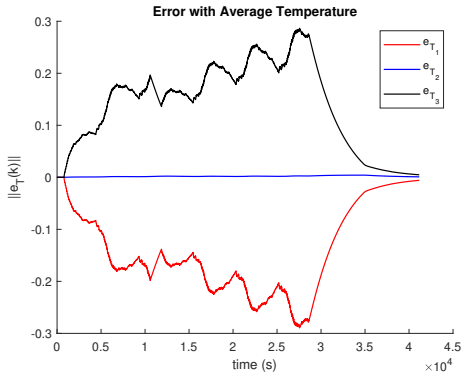

Figure 7.29: Error in Temperature among cells for Model 1 - Scenario 3

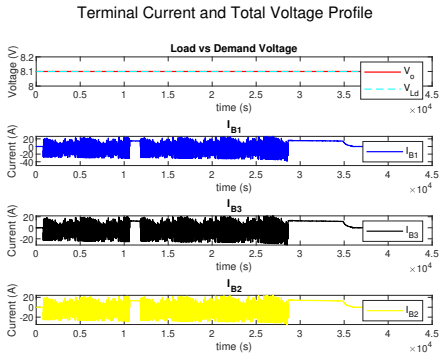

Figure 7.30: Total load voltage and cell current for Model 1 - Scenario 3

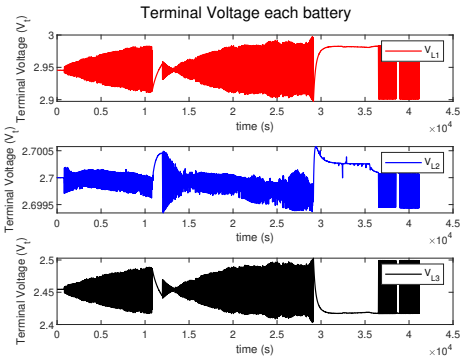

Figure 7.31: Terminal cell voltage for Model 1 - Scenario 3

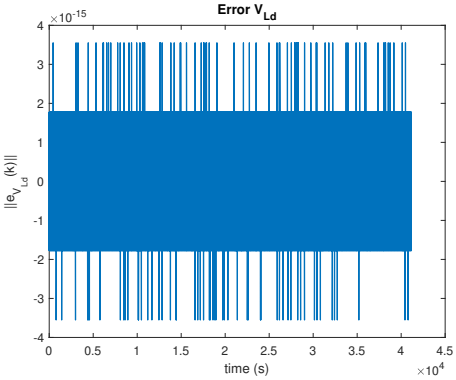

Figure 7.32: Error terminal voltage vs demand for Model 1 - Scenario 3

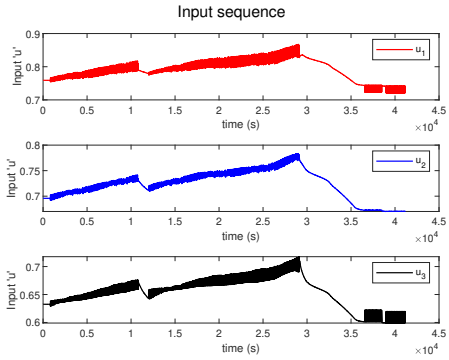

Figure 7.33: Input sequence for each cell for Model 1 - Scenario 3

7.2.1.2 Model 2

In this strategy, hard constraint on output power demand is maintained however, control move restriction has been relaxed on cells by introducing and minimizing

Parameter	Value
SOC	[0.75, 0.75, 0.65]
Temperature	[25, 25, 25] ^oC
SoR	[1, 1.2, 1.4]
SoH	[1, 0.9, 0.8]
V_{Ld}	8.1 V

Table 7.5: Model 2 experimental setup

slack variable to observe the control violations from $\Delta u = 0.1$ required by the system to fulfill the power demand at each time step in order to obtain feasible solution. The objective function for this control model is expressed in eq. (6.19). In order to create a significant contrast the initial parameters are set as shown in table 7.5:

The energy balancing is achieved very rapidly as evident from figures (7.34) and (7.36). At around 600 seconds in the drive cycle the SoC difference across cells is reduced to within ±2% limit imposed and it remains within that region throughout. Thermal behavior is same as previous cases as eminent from figures (7.35) and (7.37). The system output can be seen in figures (7.38) and (7.40). Main purpose of this experimental setup was to find a benchmark for comparison with hard constraint on control move that will be shown and section 7.2.1.3. Here it can be seen that with $\Delta u = 0.1$ the system needs to persistently violate the control move restriction as evident from figure (7.43) to achieve faster balancing and meet power demand. These violation however tend to diminish over the drive cycle once the balancing is achieved.

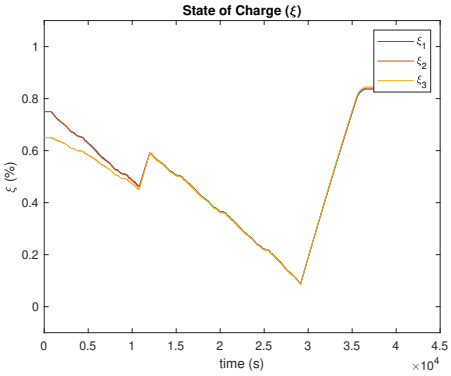

Figure 7.34: SOC for Model 2

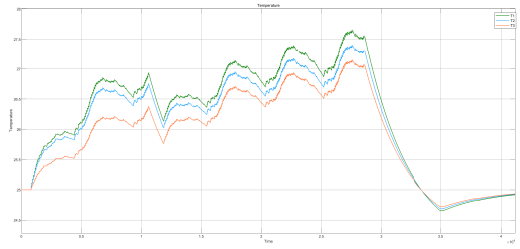

Figure 7.35: Temperature for Model 2

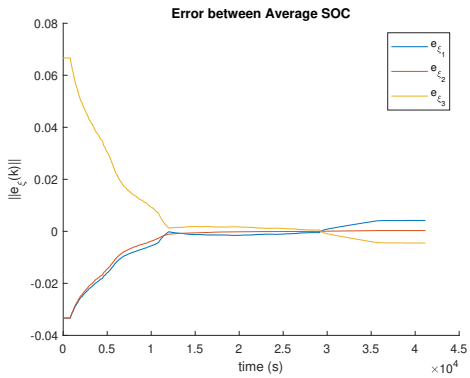

Figure 7.36: Error in SOC among cells for Model 2

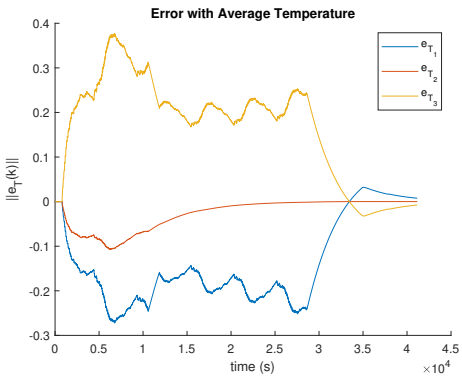

Figure 7.37: Error in Temperature among cells for Model 2

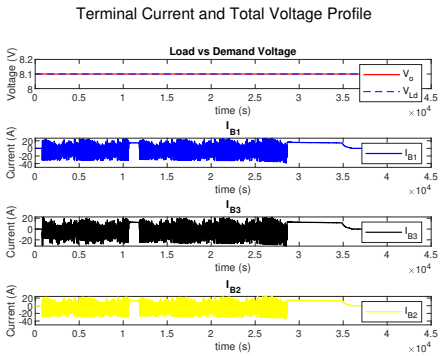

Figure 7.38: Total load voltage and cell current for Model 2

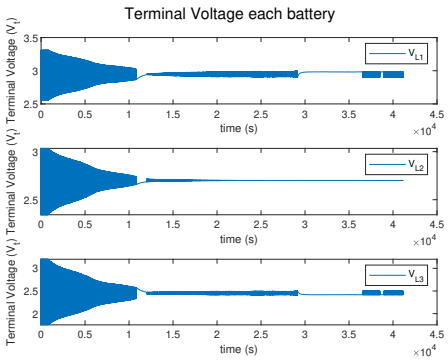

Figure 7.39: Terminal cell voltage for Model 2

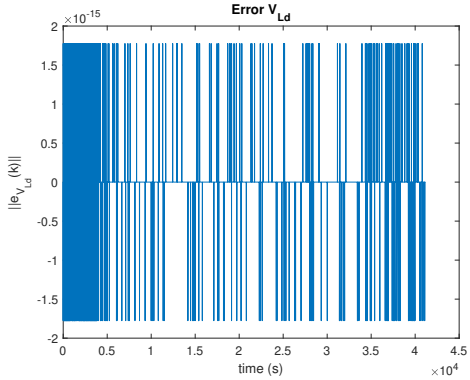

Figure 7.40: Error terminal voltage vs demand for Model 2

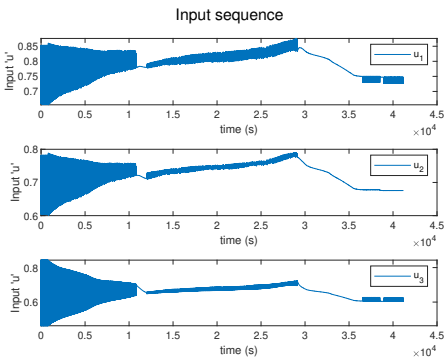

Figure 7.41: Input sequence for each cell for Model 2

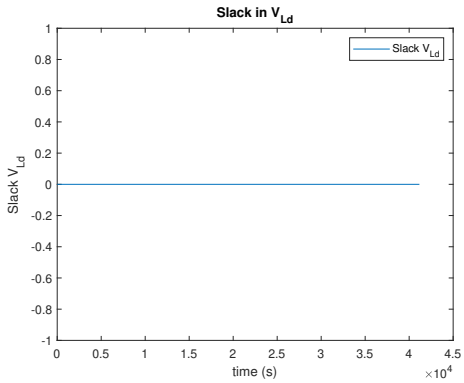

Figure 7.42: Slack variable load voltage for Model 2

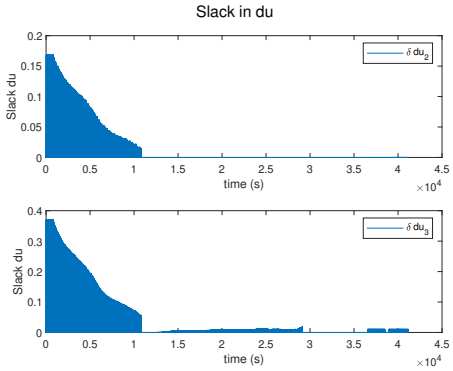

Figure 7.43: Slack variable control move for Model 2

7.2.1.3 Model 3

Here hard constraint on control move $\Delta u = 0.1$ is imposed for all the cells besides the one with maximum power capacity. However, in order to obtain a feasible solution at all time constraint on output power demand has been relaxed by introducing and minimizing slack variable accordingly. The objective function for this control model is expressed in eq. (6.20). Experimental setup is kept the same as shown in table 7.5.

It is very clear when comparing the SoC curves for model 2 (figure (7.34)) and model 3 (figure (7.44)) that the balancing is significantly slower for model 3 due to imposed control move restrictions. The system also fails to meet the demand voltage accurately as seen in figures (7.48) and (7.52), the shortfall in output increase during the long discharge cycle while it decreases towards the end when long charge cycle occurs. Contribution of cells is also been greatly affected between two scenarios with peak terminal voltages in model 3 much lower for weaker cells in figure (7.49) compared to model 2 in figure (7.40). Same is the case for input sequence (switching DC) of cells being more active in model 2 as shown in figure (7.41) compared to model 3 illustrated in figure (7.51).

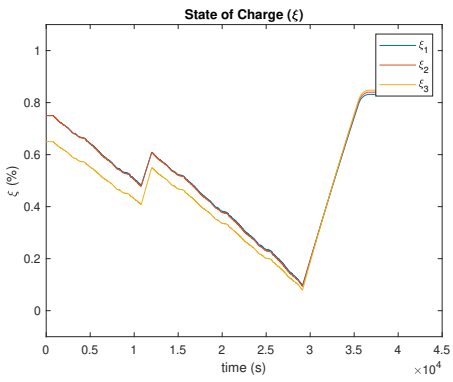

Figure 7.44: SOC for Model 3

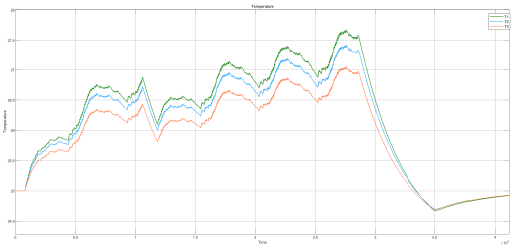

Figure 7.45: Temperature for Model 3

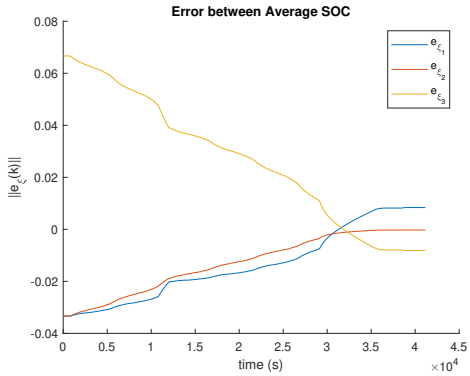

Figure 7.46: Error in SOC among cells for Model 3

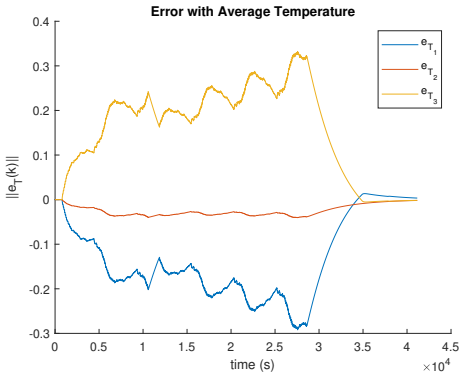

Figure 7.47: Error in Temperature among cells for Model 3

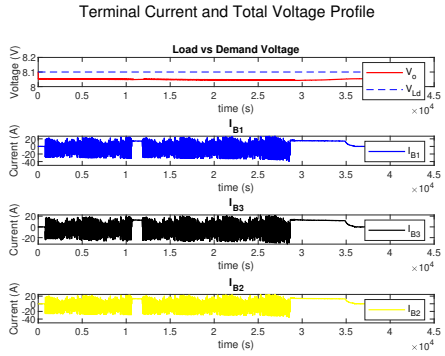

Figure 7.48: Total load voltage and cell current for Model 3

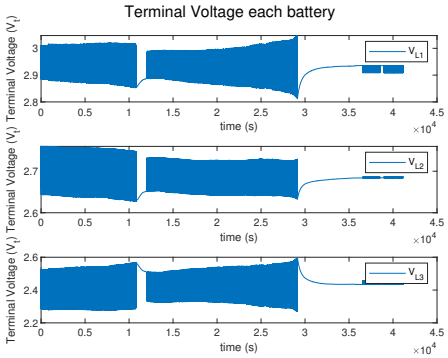

Figure 7.49: Terminal cell voltage for Model 3

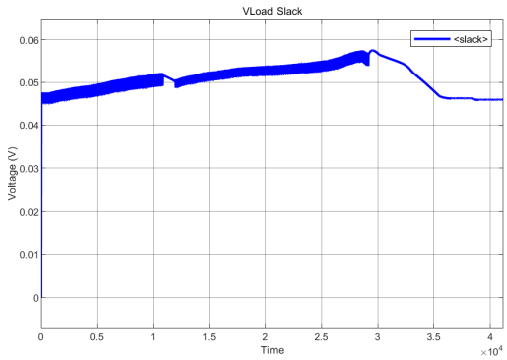

Figure 7.50: Error terminal voltage vs demand for Model 3

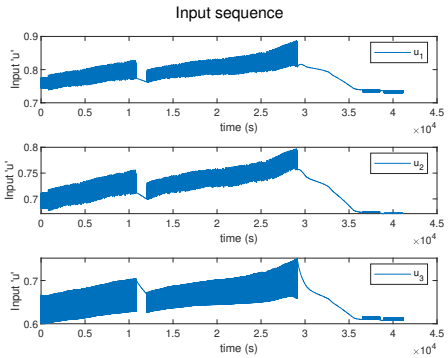

Figure 7.51: Input sequence for each cell for Model 3

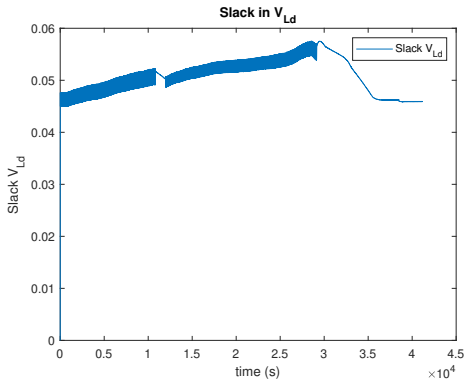

Figure 7.52: Slack variable load voltage for Model 3

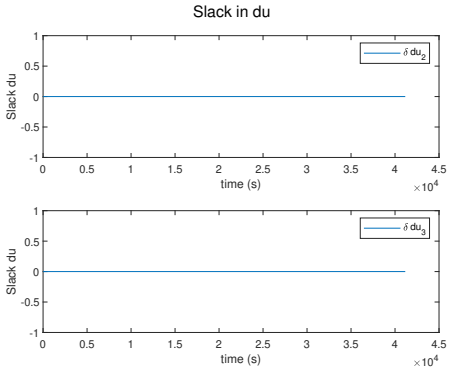

Figure 7.53: Slack variable control move for Model 3

7.3 Discussion

From the preceding sections it can be seen that RBS works much better compared to a CBS in terms of maximising systems power capabilities and achieving balancing objective. It is evident from figure (7.2) that the battery pack suffers from overcharge and/or discharge of a cell since power drawn is uniform throughout the drive cycle. This leads to optimization problem becoming infeasible at some point. On the other hand with RBS, figure (7.10) the system performs much better in meeting power demand while managing to achieve balance in states.

It was found that although a generic solution (objective function) might be able to achieve balancing as in section 7.2.1.1.2, some fine tuning based on specific system conditions can drastically improve the performance to achieve somewhat ideal performance as in section 7.2.1.1.3.

It was also observed that system with active control 7.2.1.1.3 achieve balancing much faster than the systems with control move restrictions 7.2.1.3. However still the system performance reasonably well given the control move restrictions. This can result in reducing the switching frequency for several cells inside a battery pack and lessen losses due to frequent switching. This is something that can be explored in future research.

8

Conclusion

The chapter consists of two sections. In the first section 8.1 the contributions made and research done in this thesis work is summarized. In the second section 8.2 the potential for future research work has been discussed.

8.1 Contributions

This thesis was aimed towards investigating RBS, its performance compared with CBS and finding optimal control that ensures maximization of systems power capabilities while also achieving SoC and thermal balancing. Mian contribution is summarized as follows:

1. A computationally efficient and easy to scale model for RBS has been constructed.
2. A load sharing problem has been created and investigated with main objective of minimizing the cost in (6.10) based on the model developed in Step 1 while respecting given physical constraints(dynamics, safety, health, power limits etc.) of each unit.
3. The control problem has been solved in RHC fashion using MPC framework.
4. A performance based comparison between CBS and RBS has been made.
5. An experimental study has been performed to examine system performance with control move restriction on some cells of the pack.

8.2 Future Work

This thesis work opens up several avenues for future research work some of which are highlighted as under:

- Some of the cells non linear parameters such as internal resistance and OCV were considered constant for simplicity reason. A more robust solution related to effects of these parametric variations can be conducted in future by incorporating the non-linear behavior.
- In this work only UPC has be studied in this research work. A study into using BPC can be carried out to investigate if superior performance can be achieved compared to UPC.
- Power losses and harmonics due to switching are ignored in this work for simplicity. Future works can integrate these losses and study their effect on the performance for more accurate model.

- Additional resistance present in physical system due to connecting cables has been ignored. This is acceptable if the battery packs are located very close to each other. This can be included in the design to achieve more accurate model for applications where battery packs are distant apart.
- A study can be carried out for optimal control and balancing of RBS comprising parallel packs connected with other.

Bibliography

[1] E. Nagler, "Standing still," July 2021, available at https://www.racfoundation.org/wp-content/uploads/standing-still-Nagler-June-2021.pdf.

[2] H. Weiji, Z. Changfu, Z. Liang, O. Quan, and W. Torsten, "Near-fastest battery balancing by cell/module reconfiguration," *IEEE Transactions on Smart Grid*, vol. 10, no. 6, pp. 6954–6964, 2019.

[3] "Lithium batteries: Science and technology christian julien, alain mauger, ashok vijh, and karim zaghib: Springer, 2016 619 pages, 179.00($e-book$139.00) isbn 978-3-319-19107-2," *MRS Bulletin*, vol. 41, no. 9, p. 45–45, 2016.

[4] R. Xiong, *Battery Management Algorithm for Electric Vehicles*, "1" ed. Springer, Cham and China Machine Press, 2020.

[5] H. Rahimi Eichi, U. Ojha, F. Baronti, and M.-Y. Chow, "Battery management system: An overview of its application in the smart grid and electric vehicles," *Industrial Electronics Magazine, IEEE*, vol. 7, pp. 4–16, 06 2013.

[6] A. B. Ahmad, C. A. Ooi, D. Ishak, and J. Teh, "Cell balancing topologies in battery energy storage systems: A review," in *10th International Conference on Robotics, Vision, Signal Processing and Power Applications*, M. A. M. Zawawi, S. S. Teoh, N. B. Abdullah, and M. I. S. Mohd Sazali, Eds. Singapore: Springer Singapore, 2019, pp. 159–165.

[7] E. Maiser, "Battery packaging - technology review," vol. 1597, 06 2014, pp. 204–218.

[8] U. G. Assembly, "Transforming our world : the 2030 agenda for sustainable development," 21 October 2015, available at https://www.refworld.org/docid/57b6e3e44.html.

[9] U. Nations, "Paris agreement," 2 April 2016, available at https://unfccc.int/sites/default/files/english_paris_agreement.pdf.

[10] E.-L. P. Capros, A. D. Vita, N. Tasios, D. Papadopoulos, P. Siskos, E. Apostolaki, M. Zampara, L. Paroussos, K. Fragiadakis, N. Kouvaritakis, and et al, "EU energy, transport and GHG emissions trends to 2050," 16 December 2013, available at https://ec.europa.eu/clima/sites/default/files/strategies/2030/docs/eu_trends_2050_en.pdf.

[11] Lain, J. Brandon, and E. Kendrick, "Design strategies for high power vs. high energy lithium ion cells," *Batteries*, vol. 5, p. 64, 10 2019.

[12] M. Dubarry, N. Vuillaume, and B. Y. Liaw, "Origins and accommodation of cell variations in li-ion battery pack modeling," *Int. J. Energy Res.*, vol. 34, no. 2, pp. 216–231, 2010.

[13] A. Barré, B. Deguilhem, S. Grolleau, M. Gerard, F. Suard, and D. Riu, "A review on lithium-ion battery ageing mechanisms and estimations for automotive applications," *Journal of Power Sources*, vol. 241, p. 680–689, 11 2013.

[14] J. Vetter, P. Novák, M. Wagner, C. Veit, K. Möller, J. Besenhard, M. Winter, M. Wohlfahrt-Mehrens, C. Vogler, and A. Hammouche, "Ageing mechanisms in lithium-ion batteries," *Journal of Power Sources*, vol. 147, pp. 269–281, 09 2005.

[15] J. Wang, P. Liu, J. Hicks-Garner, E. Sherman, S. Soukiazian, M. Verbrugge, H. Tataria, J. Musser, and P. Finamore, "Cycle-life model for graphite-lifepo4 cells," *Journal of Power Sources*, vol. 196, no. 8, pp. 3942–3948, 2011. [Online]. Available: https://www.sciencedirect.com/science/article/pii/S0378775310021269

[16] J. Groot, "State-of-health estimation of li-ion batteries: Ageing models," *Ph.D. dissertation, Dept. Energy Environ., Chalmers Univ. Technol., Göteborg, Sweden*, 2014. [Online]. Available: https://publications.lib.chalmers.se/records/fulltext/205605/205605.pdf

[17] M. Alahmad, H. Hess, M. Mojarradi, W. West, and J. Whitacre, "Battery switch array system with application for jpl's rechargeable micro-scale batteries," *Journal of Power Sources*, vol. 177, no. 2, pp. 566–578, 2008. [Online]. Available: https://www.sciencedirect.com/science/article/pii/S0378775307025293

[18] S. Ci, J. Zhang, H. Sharif, and M. Alahmad, "A novel design of adaptive reconfigurable multicell battery for power-aware embedded networked sensing systems," in *IEEE GLOBECOM 2007 - IEEE Global Telecommunications Conference*, 2007, pp. 1043–1047.

[19] H. Kim and K. G. Shin, "On dynamic reconfiguration of a large-scale battery system," in *2009 15th IEEE Real-Time and Embedded Technology and Applications Symposium*, 2009, pp. 87–96.

[20] T. Kim, W. Qiao, and L. Qu, "Power electronics-enabled self-x multicell batteries: A design toward smart batteries," *IEEE Transactions on Power Electronics*, vol. 27, no. 11, pp. 4723–4733, 2012.

[21] A. Barré, B. Deguilhem, S. Grolleau, M. Gérard, F. Suard, and D. Riu, "A review on lithium-ion battery ageing mechanisms and estimations for automotive applications," *Journal of Power Sources*, vol. 241, pp. 680–689, 2013. [Online]. Available: https://www.sciencedirect.com/science/article/pii/S0378775313008185

[22] X. Feng, M. Ouyang, X. Liu, L. Lu, Y. Xia, and X. He, "Thermal runaway mechanism of lithium ion battery for electric vehicles: A review," *Energy Storage Materials*, vol. 10, pp. 246–267, 2018. [Online]. Available: https://www.sciencedirect.com/science/article/pii/S2405829716303464

[23] W. H. L. ZHANG and Y. HAN, *MATHEMATICAL MODELING, PERFORMANCE ANALYSIS AND CONTROL OF BATTERY EQUALIZATION SYSTEMS: REVIEW AND RECENT DEVELOPMENTS*, 2017, pp. 281–302.

[24] F. Feng, X. Hu, J. Liu, X. Lin, and B. Liu, "A review of equalization strategies for series battery packs: variables, objectives, and algorithms," *Renewable and*

Sustainable Energy Reviews, vol. 116, p. 109464, 2019. [Online]. Available: https://www.sciencedirect.com/science/article/pii/S1364032119306720

[25] F. Altaf, L. Johannesson, and B. Egardt, "Simultaneous thermal and state-of-charge balancing of batteries: A review," in *2014 IEEE Vehicle Power and Propulsion Conference (VPPC)*, 2014, pp. 1–7.

[26] F. Altaf, B. Egardt, and L. Johannesson, "Electro-thermal control of modular battery using model predictive control with control projections," *IFAC-PapersOnLine*, vol. 48, no. 15, pp. 368–375, 2015, 4th IFAC Workshop on Engine and Powertrain Control, Simulation and Modeling E-COSM 2015. [Online]. Available: https://www.sciencedirect.com/science/article/pii/S2405896315019291

[27] C. Pinto, J. V. Barreras, E. Schaltz, and R. E. Araújo, "Evaluation of advanced control for li-ion battery balancing systems using convex optimization," *IEEE Transactions on Sustainable Energy*, vol. 7, no. 4, pp. 1703–1717, 2016.

[28] D. Docimo and H. Fathy, "Analysis and control of charge and temperature imbalance within a lithium-ion battery pack," *IEEE Transactions on Control Systems Technology*, vol. PP, pp. 1–14, 04 2018.

[29] G. K. Peprah, F. Liberati, F. Altaf, G. Osei-Dadzie, A. Di Giorgio, and A. Pietrabissa, "Optimal load sharing in reconfigurable battery systems using an improved model predictive control method," in *2021 29th Mediterranean Conference on Control and Automation (MED)*, 2021, pp. 979–984.

[30] F. Altaf, B. Egardt, and L. Johannesson Mårdh, "Load management of modular battery using model predictive control: Thermal and state-of-charge balancing," *IEEE Transactions on Control Systems Technology*, vol. 25, no. 1, pp. 47–62, 2017.

[31] F. Altaf and B. Egardt, "Comparative analysis of unipolar and bipolar control of modular battery for thermal and state-of-charge balancing," *IEEE Transactions on Vehicular Technology*, vol. 66, no. 4, pp. 2927–2941, 2017.

[32] F. Altaf, "On modeling and optimal control of modular batteries: Thermal and state-of-charge balancing," in *Ph.D. dissertation, Department of Signals and Systems Chalmers University of Technology, Gothenburg, Sweden*, 05 2016, pp. 2927–2941.

[33] Z. Zhang, Y.-Y. Cai, Y. Zhang, D.-J. Gu, and Y.-F. Liu, "A distributed architecture based on microbank modules with self-reconfiguration control to improve the energy efficiency in the battery energy storage system," *IEEE Transactions on Power Electronics*, vol. 31, no. 1, pp. 304–317, 2016.

[34] M. S. K., B. P. S., M. S. P., and M. R. N., "Intellbatt: Towards smarter battery design," in *2008 45th ACM/IEEE Design Automation Conference*, 2008, pp. 872–877.

[35] J. Andersson, "Lifetime estimation of lithiumion batteries for stationary energy storage systems," in *M.S. thesis, KTH Royal Inst. of Technology, Stockholm, Sweden*, June 2017, p. "".

[36] L. C. Casals, B. Amante García, and C. Canal, "Second life batteries lifespan: Rest of useful life and environmental analysis," *Journal of Environmental Management*, vol. 232, pp. 354–363, 2019. [Online]. Available: https://www.sciencedirect.com/science/article/pii/S0301479718313124

[37] B. Anirudh, C. Ranveer, D. Jon, F. Anthony, H. Steve, H. Pan, M. Julia, M. Thomas, P. Bodhi, and S. Evangelia, "Software defined batteries," in *Symposium on Operating Systems Principles (SOSP'15)*, October 2015.

[38] C. Zhang, K. Li, S. McLoone, and Z. Yang, "Battery modelling methods for electric vehicles - a review," *2014 European Control Conference (ECC)*, pp. 2673–2678, 2014.

[39] M. M. Hoque, M. A. Hannan, and A. Mohamed, "Voltage equalization control algorithm for monitoring and balancing of series connected lithium-ion battery," *Journal of Renewable and Sustainable Energy*, vol. 8, no. 2, p. 025703, 2016. [Online]. Available: https://doi.org/10.1063/1.4944961

[40] G. Blomgren, "The development and future of lithium ion batteries," *Journal of The Electrochemical Society*, vol. 164, pp. A5019–A5025, 01 2017.

[41] H. YONEDA, "Production technology for lithium ion secondary battery and its application to the new field," *Transactions of the Japan Society of Production Management 'Production Management'*, vol. 13, p. 27, 2007. [Online]. Available: https://ci.nii.ac.jp/naid/10026365494/en/

[42] J. C., M. A., V. A., and Z. K., *Lithium Batteries*, "" ed. Springer, Cham, 2016.

[43] Y. Jiang, C. Zhang, W. Zhang, W. Shi, and Q. Liu, "Modeling charge polarization voltage for large lithium-ion batteries in electric vehicles," *Journal of Industrial Engineering and Management*, vol. 6, 06 2013.

[44] M. Ramoni and H.-C. Zhang, "End-of-life (eol) issues and options for electric vehicle batteries," *Clean Technologies and Environmental Policy*, vol. 15, 12 2013.

[45] W. Wang, X. Wei, D. Choi, X. Lu, G. Yang, and C. Sun, *Electrochemical cells for medium- and large-scale energy storage*, 12 2015, pp. 3–28.

[46] W. Haiying, W. Feng, F. Ying, L. Ran, and Z. Qian, *Study on key technologies of lithium battery for electric vehicle*, 2011, vol. 1, pp. 291–294, 6th Int. Forum Strategic Technology (IFOST).

[47] C. Song, L. Ni, and W. Dalei, "Reconfigurable battery techniques and systems: A survey," *IEEE Access*, vol. 4, pp. 1175–1189, 2016.

[48] M. Keyser, A. Pesaran, Q. Li, S. Santhanagopalan, K. Smith, E. Wood, S. Ahmed, I. Bloom, E. Dufek, M. Shirk, A. Meintz, C. Kreuzer, C. Michelbacher, A. Burnham, T. Stephens, J. Francfort, B. Carlson, J. Zhang, R. Vijayagopal, K. Hardy, F. Dias, M. Mohanpurkar, D. Scoffield, A. N. Jansen, T. Tanim, and A. Markel, "Enabling fast charging – battery thermal considerations," *Journal of Power Sources*, vol. 367, pp. 228–236, 2017. [Online]. Available: https://www.sciencedirect.com/science/article/pii/S0378775317308819

[49] S. Li, C. C. Mi, and M. Zhang, "A high-efficiency active battery-balancing circuit using multiwinding transformer," *IEEE TRANSACTIONS ON INDUSTRY APPLICATIONS,*, vol. 49, no. 1, pp. 198–207, 2013.

[50] Y. Chen, X. Liu, Y. Cui, J. Zou, and S. Yang, "A multiwinding transformer cell-to-cell active equalization method for lithium-ion batteries with reduced number of driving circuits," *IEEE Transactions on Power Electronics*, vol. 31, pp. 4916–4929, 2016.

[51] M.-Y. Kim, C.-H. Kim, J.-H. Kim, and G. Moon, "A chain structure of switched capacitor for improved cell balancing speed of lithium-ion batteries," *IEEE Transactions on Industrial Electronics*, vol. 61, pp. 3989–3999, 2014.

[52] D. Crolla, D. E. Foster, T. Kobayashi, and N. D. Vaughan, *Encyclopedia of automotive engineering*, "1" ed. FISITA, 2015.

[53] F. Altaf, L. Johannesson, and B. Egardt, "Evaluating the potential for cell balancing using a cascaded multi-level converter using convex optimization*," *IFAC Proceedings Volumes*, vol. 45, no. 30, pp. 100–107, 2012, 3rd IFAC Workshop on Engine and Powertrain Control, Simulation and Modeling. [Online]. Available: https://www.sciencedirect.com/science/article/pii/S1474667015351454

[54] Y. Li, M. Vilathgamuwa, T. Farrell, S. S. Choi, N. Tran, and J. Teague, "A physics-based distributed-parameter equivalent circuit model for lithium-ion batteries," *Electrochimica Acta*, vol. 299, pp. 451–469, 03 2019.

[55] Y. Hu, B. Yurkovich, S. Yurkovich, and Y. Guezennec, "Electro-thermal battery modeling and identification for automotive applications," *Proc. ASME Dyn. Syst. Control Conf.*, 01 2009.

[56] B. Yurkovich and Y. Guezennec, "Lithium ion dynamic battery pack model and simulation for automotive applications," 01 2009.

[57] S. S. Madani, E. Schaltz, and S. Kær, "An electrical equivalent circuit model of a lithium titanate oxide battery," *Batteries*, vol. 5, p. 31, 03 2019.

[58] L. Lu, X. Han, L. Jianqiu, J. Hua, and M. Ouyang, "A review on the key issues for lithium-ion battery management in electric vehicles," *Journal of Power Sources*, vol. 226, p. 272–288, 03 2013.

[59] F. P. Incropera and D. P. DeWitt, *Fundamentals of Heat and Mass Transfer*, 4th ed. New York City, New York: John Wiley and Sons, Inc., 1996.

[60] S. Blundell, K. Blundell, and O. Narayan, "Concepts in thermal physics," *Physics Today - PHYS TODAY*, vol. 60, 10 2007.

[61] M. Shen and Q. Gao, "A review on battery management system from the modeling efforts to its multiapplication and integration," *International Journal of Energy Research*, vol. 43, 04 2019.

[62] W. C. Lee, D. Drury, and P. Mellor, "Comparison of passive cell balancing and active cell balancing for automotive batteries," *2011 IEEE Vehicle Power and Propulsion Conference*, pp. 1–7, 2011.

[63] R. Mahamud and C. Park, "Reciprocating air flow for li-ion battery thermal management to improve temperature uniformity," *Lancet*, vol. 196, pp. 5685–5696, 07 2011.

[64] L. Lam, P. Bauer, and E. Kelder, "A practical circuit-based model for li-ion battery cells in electric vehicle applications," *Telecommunications Energy Conference (INTELEC), 2011 IEEE 33rd International*, pp. 1–9, 10 2011.

[65] X. Lin, A. Stefanopoulou, H. Perez, J. Siegel, Y. Li, and D. Anderson, "Quadruple adaptive observer of the core temperature in cylindrical li-ion batteries and their health monitoring," 06 2012, pp. 578–583.

[66] A. Žukauskas, "Heat transfer from tubes in crossflow," ser. Advances in Heat Transfer, J. P. Hartnett and T. F. Irvine, Eds. Elsevier, 1972, vol. 8, pp.

93–160. [Online]. Available: https://www.sciencedirect.com/science/article/pii/S0065271708700388

[67] Z. B. Omariba, L. Zhang, and D. Sun, "Review of battery cell balancing methodologies for optimizing battery pack performance in electric vehicles," *IEEE Access*, vol. 7, pp. 129 335–129 352, 2019.

[68] S. Al-Hallaj, J. Prakash, and J. Selman, "Characterization of commercial li-ion batteries using electrochemical–calorimetric measurements," *Journal of Power Sources*, vol. 87, p. 186–194, 04 2000.

[69] X. Lin, H. Perez, S. Mohan, J. Siegel, A. Stefanopoulou, Y. Ding, and M. Castanier, "A lumped-parameter electro-thermal model for cylindrical batteries," *Journal of Power Sources*, vol. 257, p. 1–11, 07 2014.

[70] K. Smith and C.-Y. Wang, "Power and thermal characterization of a lithium-ion battery pack for hybrid-electric vehicles," *Journal of Power Sources*, vol. 160, pp. 662–673, 09 2006.

[71] S. Wang, "Entropy and heat generation of lithium cells/batteries," *Chinese Physics B*, vol. 25, p. 010509, 01 2016.

[72] V. Srinivasan and C. Wang, "Analysis of electrochemical and thermal behavior of li-ion cells," *Journal of The Electrochemical Society*, vol. 150, 2003.

[73] J. Lempert, P. Kollmeyer, P. Malysz, O. Gross, J. Cotton, and A. Emadi, "Battery entropic heating coefficient testing and use in cell-level loss modeling for extreme fast charging," 04 2020.

[74] A. Iserles, U. Iserles, D. Crighton, M. Ablowitz, S. Davis, E. Hinch, J. Ockendon, C. Crighton, and P. Olver, *A First Course in the Numerical Analysis of Differential Equations*, ser. Cambridge Texts in Applied Mathematics. Cambridge University Press, 1996. [Online]. Available: https://books.google.se/books?id=obqCyAs0BssC

[75] S. Ma, M. Jiang, P. Tao, C. Song, J. Wu, J. Wang, T. Deng, and W. Shang, "Temperature effect and thermal impact in lithium-ion batteries: A review," *Progress in Natural Science: Materials International*, vol. 28, no. 6, pp. 653–666, 2018. [Online]. Available: https://www.sciencedirect.com/science/article/pii/S1002007118307536

[76] "Power capability prediction for lithium-ion batteries using economic nonlinear model predictive control," *Journal of Power Sources*, vol. 396, pp. 580–589, 2018. [Online]. Available: https://www.sciencedirect.com/science/article/pii/S037877531830630X

[77] Y. Barsukov and T. Instruments, "Battery cell balancing: What to balance and how," 07 2021.

[78] D. Linden and T. B. Reddy, *Linden's Handbook of Batteries*, 3rd ed. McGraw-Hill, 2011.

[79] J. Löfberg, "Yalmip : A toolbox for modeling and optimization in matlab," in *In Proceedings of the CACSD Conference*, Taipei, Taiwan, 2004.

[80] H. Arasaratnam, J. Tjong, and S. Habibi, "Switched-capacitor cell balancing: A fresh perspective," *SAE Technical Papers*, vol. 1, 04 2014.

A

Appendix 1

A.1 System Matrices

The matrices for the model shown in (5.22) on page 31 are as under:

$$\dot{x}(t) = \underbrace{\begin{bmatrix} A_E & 0 & 0 \\ 0 & A_{V_1} & 0 \\ 0 & 0 & A_T \end{bmatrix}}_{A} \underbrace{\begin{bmatrix} \xi(t) \\ V_1(t) \\ T(t) \end{bmatrix}}_{x(t)} + \underbrace{\begin{bmatrix} B_E \\ B_{V_1} \\ B_T \end{bmatrix}}_{B} u(t) + \underbrace{\begin{bmatrix} 0 & 0 \\ 0 & 0 \\ E_{T_f} & E_{T_{amb}} \end{bmatrix}}_{E} \begin{bmatrix} T_f \\ T_{amb} \end{bmatrix}$$

$$y(t) = \begin{bmatrix} T(t) \\ V_L(t) \end{bmatrix} = \underbrace{\begin{bmatrix} 0 & 0 & 1 \\ 0 & 0 & 0 \end{bmatrix}}_{C} x(t) + \underbrace{\begin{bmatrix} 0 \\ D_V \end{bmatrix}}_{D} u(t)$$

B

List of Acronyms

Abbreviation	Full Form
SoP	State of Power
SoC	State of Charge
SOH	State of Health
SoR	State of Resistance
EoL	End of Life
RuL	Remaining Useful Life
OCV	Open Circuit Voltage
ECM	Equivalent Circuit Model
KCL	Kirchhoff's Current Law
KVL	Kirchhoff's Voltage Law
DC	Duty Cycle
PWM	Pulse Width Modulation
UDC	Uniform Duty Cycle
MPC	Model Predictive Control
LiB	Lithium ion Battery
BMS	Battery Management System
PU	Power Unit
DAE	Differential Algebraic Equation
PDAE	Partial Differential Algebraic Equation
UPC	Uni-Polar Control
BPC	Bi-Polar Control

DEPARTMENT OF ELECTRICAL ENGINEERING
CHALMERS UNIVERSITY OF TECHNOLOGY
Gothenburg, Sweden
www.chalmers.se

CHALMERS
UNIVERSITY OF TECHNOLOGY